

Parvulin-type PPIase, PrsA, contributes to folding and stability of virulence factors that determine pathogenicity in Gram-positive bacteria

by

Madeline Torres

B.S., University of Delaware, 2018

Submitted to the Graduate Faculty of the
Dietrich School of Arts and Sciences in partial fulfillment
of the requirements for the degree of
Master of Science

University of Pittsburgh

2022

UNIVERSITY OF PITTSBURGH

DIETRICH SCHOOL OF ARTS AND SCIENCES

This thesis was presented

by

Madeline L. Torres

It was defended on

November 29, 2022

and approved by

Jacob D. Durrant, Ph.D., Associate Professor, Biological Sciences

Andrea J. Berman, Ph.D., Associate Professor, Biological Sciences

Jon P. Boyle, Ph.D., Professor, Biological Sciences

Thesis Advisor: Laty A. Cahoon, Ph.D., Assistant Professor, Biological Sciences

Copyright © by Madeline L. Torres

2022

Parvulin-type PPIase, PrsA, contributes to folding and stability of virulence factors that determine pathogenicity in Gram-positive bacteria

Madeline L. Torres, M.S.

University of Pittsburgh, 2022

During host infection, post-translocational molecular chaperones in Gram-positive bacteria function to regulate secreted virulence factors. These virulent proteins are secreted in an unfolded state and in order to contribute to pathogenesis, they must be properly folded. One chaperone, named PrsA, is present in many pathogenic Gram-positive bacteria and contributes to the ability of those bacteria to infect their hosts. The mechanisms in which PrsA proteins stabilize and facilitate the full functionality of their client proteins are largely understudied. Therefore, I used Gram-positive bacteria *Listeria monocytogenes* (*Lm*) and *Streptococcus pneumoniae* (*Sp*) as model bacterial organisms to uncover these molecular mechanisms. During host cell infection, *L. monocytogenes* and *S. pneumoniae* secrete virulence factors across the bacterial membrane, to an area between the membrane and cell wall. This interface is solvent accessible and may expose secreted proteins to a harsh environment problematic for protein folding. PrsA proteins, which function as post-translocational molecular chaperones and PPIases, are present in the cell wall-membrane interface of Gram-positive bacteria and I hypothesize PrsA is responsible for the full functionality and stability of secreted virulence proteins. Here, I present my findings of the relationship between the pore-forming toxins listeriolysin-O (LLO) and pneumolysin (Ply) with *LmPrsA2* and *SpPrsA*, respectively. Our data shows that *LmPrsA2* and *SpPrsA* interact with many virulence factors, and despite the loss of the entire PPIase domain, they can retain strong interactions with LLO and Ply, which are thought to be folded by the PPIase and/or foldase domains. Our data highlight the potential for an antimicrobial candidate capable of decreasing the

spread and growth of *Lm* and *Sp* by inhibiting the hydrophobic binding pocket of the PrsA foldase domain.

Table of Contents

PREFACE	0
1.0 INTRODUCTION.....	1
1.0 GRAM-POSITIVE BACTERIA	1
1.0.1 THREATS TO PUBLIC HEALTH.....	2
1.0.2 ANTIMICROBIAL RESISTANCE	4
1.1 CHAPERONES AND PPIASES	5
1.1.1 BIOLOGICAL FUNCTION	5
1.1.2 CHAPERONES AND PPIASE IN GRAM-POSITIVE BACTERIA	6
1.1.3 ROLE OF PPIASES IN DRUG DISCOVERY	7
1.2 PRSA AND ORTHOLOGS	8
1.2.1 STRUTURES, HOMOLOGY, AND SIMILARITY	8
1.2.2 KNOWN FUNCTIONS IN VIRULENCE AND CELULAR PROCESSES	9
2.0 CHARACTERIZATION OF PRSA INTERACTIONS WITH VIRULENCE FACTORS OF GRAM-POSITIVE BACTERIA	10
2.0 INTRODUCTION	10
2.1 PORE-FORMING TOXINS AND GRAM-POSITIVE BACTERIAL PRSAS	12
2.1.1 IDENTIFICATION OF LLO AND PLY WITH <i>LM</i>PRSA2 AND <i>SPP</i>PRSA	12
2.2 IDENTIFICATION OF VARIOUS INTERACTING PARTNERS OF <i>LM</i>PRSA2 AND <i>SPP</i>PRSA	15

2.2.1 COLABFOLD AS A METHOD TO IDENTIFY PROTEIN-PROTEIN INTERACTIONS.....	18
2.3 DISCUSSION	19
2.4 FUTURE DIRECTIONS	20
3.0 IDENTIFYING THE ACTIVE DOMAINS WITHIN PRSA PROTEINS	22
3.0 INTRODUCTION	22
3.0.1 THE PPIASE AND FOLDASE DOMAINS.....	22
3.0.2 OVERLAPS IN FUNCTIONS OF PRSAS	23
3.1 IDENTIFICATION OF FUNCTIONAL REGIONS OF LMPRSA2 AND SPPRSA	24
3.2 PRSA AS A THERAPEUTIC TARGET	28
3.3 DISCUSSION	29
3.4 FUTURE DIRECTIONS	30
4.0 MATERIALS AND METHODS	32
4.0 PROTEIN PURIFICATION	32
4.1 MICROSCALE THERMOPHORESIS (MST)	35
4.2 AFFINITY ISOTHERMAL TITRATION CALORIMETRY (ITC)	35
4.3 PROTEIN COMPLEX STRUCTURE PREDICTION	36
4.4 STABLE ISOTOPE LABELING OF AMINO ACIDS IN CELL CULTURE (SILAC) PULLDOWN	37
BIBLIOGRAPHY	39

List of Figures

Figure 1. Anatomy of Gram-positive bacterial envelope.	2
Figure 2. <i>Lm</i> route of infection.	3
Figure 3 <i>Sp</i> mode of infection.	4
Figure 4. Structural and sequence alignment of <i>LmPrsA2</i> and <i>SpPrsA</i>.....	8
Figure 5. Schematic of post-translocational protein folding in <i>Lm</i> and <i>Sp</i>.	11
Figure 6. MST of <i>LmPrsA2</i> and <i>SpPrsA</i> with LLO and Ply.....	13
Figure 7. PrsA proteins with pore-forming cytolysins	14
Figure 8. ColabFold Structure of <i>LmPrsA2</i> with InlC and ActA.....	16
Figure 9. ColabFold Structure of <i>SpPrsA</i> with PBP2B and NanA.	17
Figure 10. PrsA N+C Mutants with LLO and Ply	25
Figure 11. <i>LmPrsA2</i> N+C Mutant with LLO	26
Figure 12. Colab Structure of <i>SpPrsA</i> N+C Mutant with Ply	27
Figure 13. Targeting PrsA Inhibition.....	28
Figure 14 Predicted Alignment Error of Protein Complex	37

PREFACE

I would like to write in thanks for the plethora of mentorship I've received over the past 3.5 years. At the beginning of my academic career, I would have never imagined growing so much as a scientist, especially in my abilities to think critically and innovatively. For that, I must attribute that to certain faculty members, including Laty, Sarah, and Andrea. Thank you to my wonderful lab mates Jada and Charles for always being willing to talk science and lighten up the lab space. There were truly never any dull moments in the Cahoon Lab.

I would also like to send my gratitude to fellow graduate students, Vero and Karen, for lending a hand whenever I was in need of emotional support (or proofreading my comps document). The diversity brunches with Elizabeth, Jahree, Aigbe, Vero and Karen helped me decompress through the first years before the pandemic struck. You are all amazing, confident women and I look up to you all! And lastly, my biggest and final thanks goes to my wonderful partner, Darian. I truly believe I wouldn't have made it this far without your unwavering support, love, and patience.

1.0 INTRODUCTION

1.0 GRAM-POSITIVE BACTERIA

First characterized by a crystal violet hue in a Gram-stain, Gram-positive bacteria have a thick peptidoglycan layer ranging from 20-80nm in length which envelopes the entire cell¹. Despite only having a single bacterial membrane compared to two in Gram-negative, Gram-positive bacteria can survive in similarly harsh conditions as Gram-negative bacteria due to the protection by the thick peptidoglycan layer, as known as the bacterial cell wall (Figure 1). The peptidoglycan cell wall has repeated teichoic acid polymers which account for about 60% of the cell wall and are either covalently bonded to peptidoglycan or anchored to the bacterial membrane^{1,2}. The presence of many teichoic acids in the cell wall and cell wall-plasma membrane interface leaves a dense, anionic charge in this area(Figure 1) and can present some challenges regarding secreted protein stability^{2,3}. In many Gram-positive bacteria, virulence factors are translocated from the cytosol across the bacterial membrane through the Sec secretion system. Proteins secreted through the Sec transport system are unfolded, due to the small size of the Sec transporter, and must remain unfolded until they are in the cell wall- bacterial membrane interface^{4,5}. Here, it is essential for them to be folded and stabilized to perform their specific task(s), such as promoting host infection or cell wall biogenesis⁴⁻⁶. Issues, such as protein aggregation, can arise here due to this area being exposed to the extracellular environment and from the dense negative charge from the cell wall. The process in which unfolded virulence proteins are fully folded in this bacterial membrane – cell wall interface is widely under characterized in most Gram-positive bacteria.

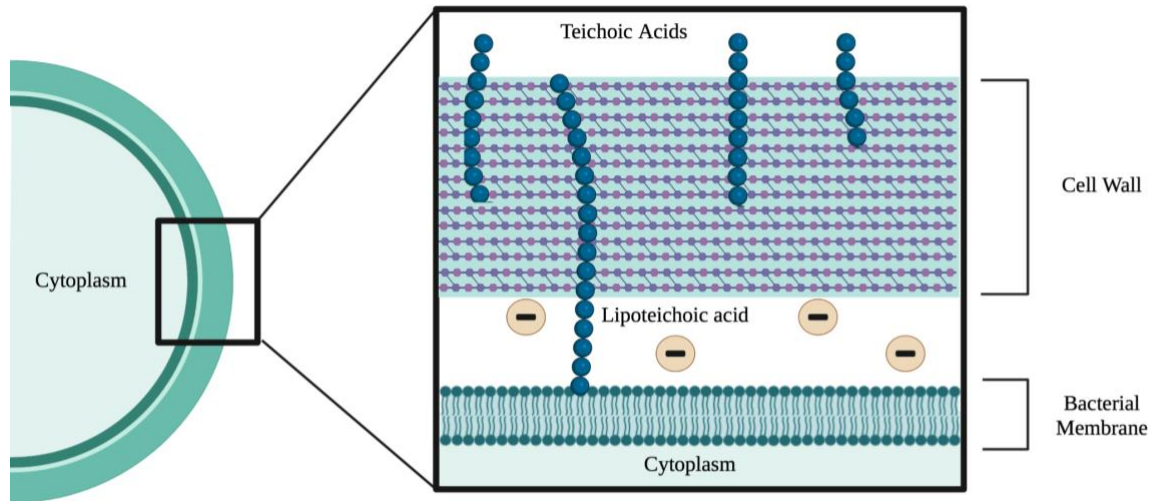


Figure 1. Anatomy of Gram-positive bacterial envelope.

Gram-positive bacteria have thick, peptidoglycan cell wall and a single bacterial membrane. In the cell wall, the presence of teichoic acids creates a negatively charged environment. Image made in BioRender.

1.0.1 THREATS TO PUBLIC HEALTH

Listeria monocytogenes (*Lm*) has a high mortality rate for vulnerable populations, such as pregnant women and children, even after antibiotic treatment in the late stages of infection, especially for those who are immunocompromised⁷. In immunocompromised individuals, once *Lm* is ingested via contaminated food, it can navigate the digestive track where it penetrates the epithelial layer of the small intestines. The onset of infection is the medley of virulence factors, internalin A and B, that are secreted to allow for host cell adhesion which propagates host cell entry, eventually leading to *Lm* vacuolar escape⁸. Once it escapes phagocytosis, *Lm* can freely replicate in the cytoplasm, ultimately allowing it to hijack host actin to further spread into neighboring cells (Figure 2). The continuation of this cycle in immunocompromised people without intervention can lead to meningitis, bacteremia, myocarditis, and spontaneous abortion in pregnant individuals⁸⁻¹⁰. Because *Lm* is capable of infecting virtually every cell in the human body,

it is a dangerous pathogen causing billions of dollars in total costs annually for medical treatment for people in the United States alone¹¹.

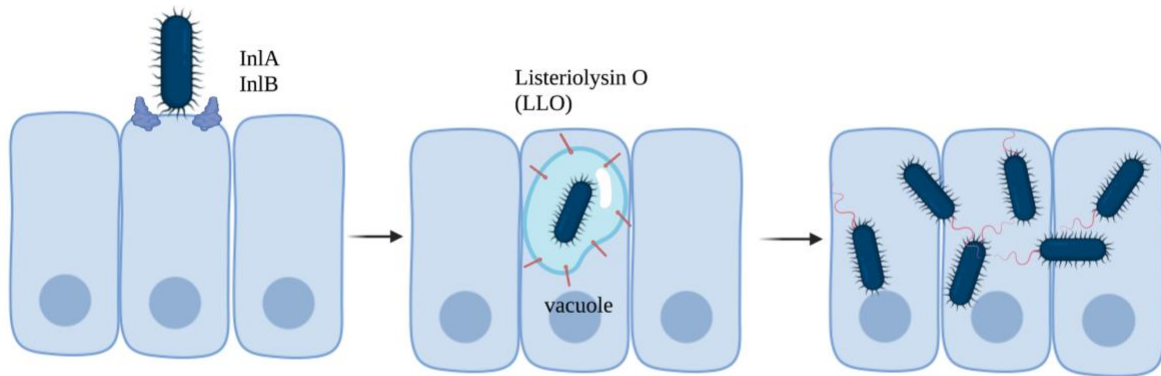


Figure 2. *Lm* route of infection.

Lm begins infection by secreting adhesions, InlA and InlB, that attach it to the host cell. This allows *Lm* to enter the cell, but the host cell places it within a vacuole for phagocytosis. A pore-forming toxin, LLO, forms pores within the host cell vacuole to allow *Lm* escape, where it can freely replicate and invade neighboring cells. Image made in Biorender.

The *Streptococcus* genus is composed of at least 49 species of Gram-positive bacteria that can colonize humans and other animals¹². Although most streptococci are commensal, meaning they are able to live in human host without harming their health, some species can cause fatal human infections such as pneumonia, sepsis, meningitis, endocarditis, and necrotizing fasciitis¹³. A primary streptococcal invasive pathogen is *Streptococcus pneumoniae* (*Sp*) and it is the leading cause of lower respiratory tract infections in the world¹⁴. During infection, streptococcal species adhere to epithelial cells lining the respiratory tract where they act primarily as an extracellular pathogen by secreting virulence factors, such as the pneumococcal surface proteins, that allow colonization¹⁵ (Figure 3). In immunocompromised individuals, *Sp* replication will continue until

the pathogen has spread to other tissues that cause diseases, such as bacteremia or meningitis. In the United States, there are an estimated 2 million *Sp* infections and more than 6,000 deaths each year¹⁶. In 2004, it was reported that pneumococcal disease contributed to \$2.4 billion worth of medical expenses in the United States alone, and is predicted to increase economic burden by an additional \$2.5 billion annually^{17,18}

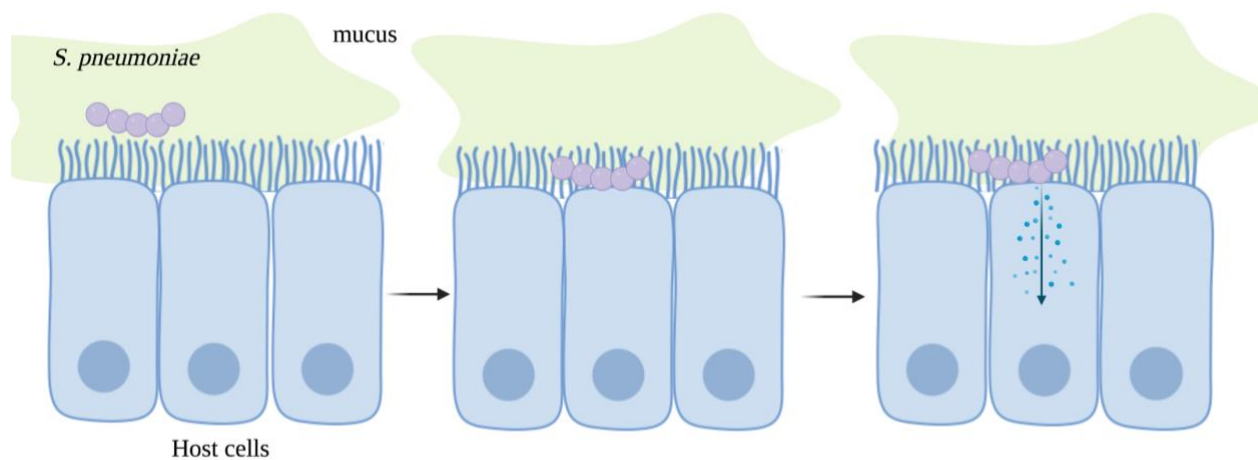


Figure 3 *Sp* mode of infection.

Once *Sp* enters the upper respiratory tract, it adheres to the epithelium lining the airways. After it adheres to the host cell surface mediated by virulence factors in its capsule, it functions extracellularly and secretes virulence factors within the host cell that allow host cell infection. Image made in Biorender.

1.0.2 ANTIMICROBIAL RESISTANCE

More than a century after the first antimicrobial, Salvarsan, was developed, Gram-positive bacterial infections still pose as a threat despite modern antimicrobials¹⁹. Antimicrobial resistance is a world-wide public health threat endangering the lives of vulnerable people globally^{11,20,21} and

has been declared by the World Health Organization (WHO) as a serious threat that requires a prompt response. Unfortunately, all antibiotics have at least one pathogenic bacterium that is resistant to them due to the rapid adaptability of many bacteria, urging many patients to find alternative treatment methods such as antivirulence drugs²². About 58,000 people die each year from Gram-positive infections in the US, with the immunocompromised, elderly, or pregnant individuals at especially high risk². Alternate treatment of Gram-positive bacteria proves to be difficult because of how little is known about the mechanisms of biomolecular trafficking in and out of the bacterial cell. Targeting mechanisms of protein folding outside of the bacterial cytosol deems valuable as this is how many pathogens establish virulence^{23,24}. Despite the lack of information on how to halt Gram-positive growth and infection, there is a growing interest in inhibiting bacterial PPIases as a potential therapeutic based on investigations inhibiting Pin1, a PPIase in humans, with the drug juglone, but this has not proven as a valuable drug in trials²⁵.

1.1 CHAPERONES AND PPIASES

1.1.1 BIOLOGICAL FUNCTION

Molecular chaperones are proteins that function to assist in the protein folding process, ultimately to speed up the folding rate and prevent aggregation of misfolded proteins²⁶. These chaperones can be ATP dependent or independent but are all highly dynamic proteins capable of shifting through many conformations to properly fold or refold their clients. A subset of molecular chaperones that have an additional folding mechanism are called peptidyl prolyl isomerases (PPIases) and they can accelerate the *cis-to-trans* isomerization of residues that are N-terminal to proline to further speed the protein folding process by 100-fold²⁷. PPIases are ubiquitously

expressed in prokaryotes and eukaryotes and typically exist to fold proteins, rather than degrade them²⁸⁻³³. There are three distinct families of PPIases: cyclophilins, FK506 binding proteins (FKBPs), and parvulins, and they are involved in diverse biological mechanisms, such as gene regulation to signal transduction^{27,34,35}. Their roles in these various processes can be partially attributed to their ability to localize to many different regions within a eukaryotic cell, such as the nucleus and mitochondria, or outside of the cell post secretion^{27,36,37} and their differential expression during cellular stress³⁸ or infection³⁹.

1.1.2 CHAPERONES AND PPIASE IN GRAM-POSITIVE BACTERIA

In bacteria, PPIases have primarily been investigated for their role during secretion and translation²⁷ but most research concerning PPIases in bacteria focuses on cyclophilins and FKBPs, so our knowledge of parvulins is currently limited. FKBPs in bacteria are characterized by an α -helix wrapped by a β -sheet with five strands. Trigger factor (TF) is the only studied FKBP in Gram-positive bacteria and it is involved in the *B. subtilis* and *L. monocytogenes* responses to cellular stress^{24,27,35,40,41}. Whereas cyclophilins possess an eight stranded anti-parallel β -barrel characterized for the ability to bind to the immunosuppressive drug cyclosporine A²⁹. Cyclophilins found in Gram-positive bacteria include PpiA and PpiB, which can function extracellularly or intracellularly respectively, and are involved in transportation of secreted proteins⁴²⁻⁴⁴. Lastly, parvulins are the most recently classified PPIase family and are characterized by a β -barrel comprising of four anti-parallel strands, making it the smallest functioning PPIase²⁸. An example of a parvulin domain-containing protein commonly found in Gram-positive bacteria includes PrsA (also known as PpmA)⁴⁵, which in addition to a PPIase domain contains a foldase domain⁴⁶ and is under investigation for its roles in bacterial virulence^{46,47}.

1.1.3 ROLE OF PPIASES IN DRUG DISCOVERY

PPIases are known to be upregulated during infection in *L. monocytogenes*, but only cyclophilins and FKBP respond to immunosuppressive drugs⁴⁸⁻⁵⁰, while parvulins can be inhibited by 5-hydroxy-1,4-naphthoquinone (juglone) and are not classified as an immunophilin, which is a PPIase that binds to immunosuppressants^{25,51}. Current research investigating an alternative method to antibiotics for bacterial infections largely involves targeting protein folding. Thus far in *Lm*, a TF deletion yields a significant defect in bacterial survival in mice spleen and livers, but most research involving the potential of FKBP as a therapeutic target has been performed in Gram-negative bacteria²⁴. Cyclophilin PpiA, also known as SlrA, is surface exposed in *Sp* and important for colonization in mammalian cells. In an *Sp* infection model, a deletion of SlrA increased mouse survival; however, Gram-positive bacteria *C. difficile* and *S. aureus* with deletions in cytoplasmic cyclophilin *ppiB* exhibit a milder reduction in virulence or functional virulence factors^{52,53}. Because parvulins do not respond to immunosuppressants, a parvulin inhibitor may be ideal for patients who are already immunocompromised or taking an immunosuppressant while fighting a bacterial infection. Current parvulin inhibitors target human Pin1 only, but no existing inhibitors of Pin1 has reached clinical trials due to the lack of stability, cell permeability, potency, and selectivity of the drugs^{24,37}. Parvulins offer a potential avenue for the treatment of pathogenic bacteria, but difficulties arise in the search for a model inhibitor. Potential bacterial parvulin inhibitors must be selective enough to avoid interference with human Pin1^{54,55}, while being effective across many Gram-positive pathogens, and especially those with antibiotic-resistance.

1.2 PRSA AND ORTHOLOGS

1.2.1 STRUCTURES, HOMOLOGY, AND SIMILARITY

A parvulin protein commonly seen across Gram-positive pathogens, called PrsA, has a broad spectrum of functions and is implicated to be important for bacterial processes ranging from cellular stress responses and virulence. Within *Lm* and *Sp*, the parvulin domain varies from organism to organism, especially in the PPIase signature motif which approximately spans residues 173-194 but overall, the two PrsAs share about 60% sequence similarity (Figure 4). Both isoforms of *Lm* PrsA (PrsA1 and PrsA2) exhibit PPIase activity, but *Sp*PrsA demonstrate no PPIase activity^{45,56}. In terms of structure, many PrsA proteins oligomerize at high concentration and form dimers *in vivo* so that they can perform their role in ethanol resistance, antibiotic resistance, stress tolerance, and other biological functions⁵⁷⁻⁶⁰. The structure of PrsA in *Sp*, *Lm*, *B. subtilis*, *S.*

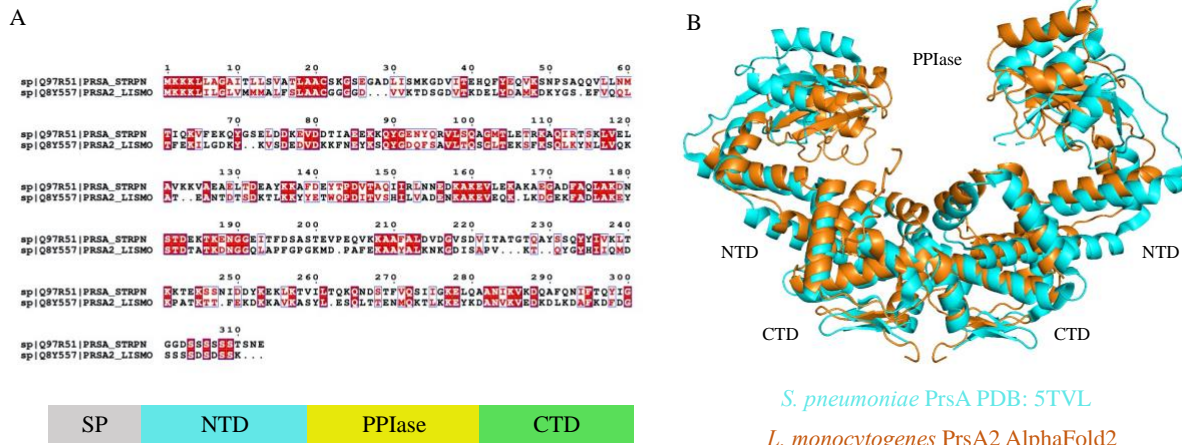


Figure 4. Structural and sequence alignment of *Lm*PrsA2 and *Sp*PrsA.

A) Multiple sequence alignment in PROMALS3D (Pei *et al.* 2008). Highlighted amino acids in alignment correspond to domain listed below of corresponding color. B) Structural alignment using *Sp*PrsA (PDB: 5TVL) and ColabFold (Mirdita *et al.* 2022) predicted structure of *Lm*PrsA2.

mutans, *B. anthracis* and other Gram-positive bacteria have been solved which exhibit PrsA in a dimer or monomer except for *SpPrsA*, which has been crystallized as a tetramer (PDB 5TVL) or dimer of dimers. We speculate that the presence of *SpPrsA* in its tetrameric form shows the protein may fold itself, but the existence of other PrsAs as dimers in their crystal structures provides further evidence that PrsA chaperones may exist primarily as dimeric foldases at physiological concentrations.

1.2.2 KNOWN FUNCTIONS IN VIRULENCE AND CELULAR PROCESSES

Observed in *L. monocytogenes* PrsA1 and PrsA2, dimer formation is necessary for full PrsA function^{57,60} (Cahoon, unpublished). *LmPrsA2*, and not *LmPrsA1*, is critical for hemolytic activity, and virulence in a murine mouse model^{59,61}. *LmPrsA1* displays PPIase activity and is important in ethanol resistance⁶⁰ and contributes to bacterial viability during the early stages of infection⁶². On the other hand, despite the lack of PPIase activity, *SpPrsA* deletions result in significant defects in virulence^{45,56}, suggesting that the foldase domain plays an important role in virulence. *SpPrsA* is critical for colonization and invasive disease^{56,63} and is conserved in *Sp* serotypes despite lacking key residues important for PPIase activity^{45,63,64}. Other streptococcal PPIases, such as *S. mutans* PrsA, are required for cell wall/membrane integrity⁶⁵ and virulence in an infective endocarditis model³¹. In this thesis, I will examine the roles of *LmPrsA2* and *SpPrsA* in interactions with virulence factors and which domain(s) are necessary for this interaction.

2.0 CHARACTERIZATION OF PRSA INTERACTIONS WITH VIRULENCE FACTORS OF GRAM-POSITIVE BACTERIA

2.0 INTRODUCTION

LmPrsA2 is a lipoprotein containing a parvulin and a foldase domain and has become a point of interest in research due to its subsequent role in establishing bacterial virulence. After secretion from the cytosol, *LmPrsA2* localizes to the bacterial membrane in the cell wall-bacterial membrane interface to help fold and stabilize other secreted and unfolded proteins⁶⁶⁻⁶⁸. The importance of *LmPrsA2* in virulence begs the question: *why* is it necessary for pathogenesis? By investigating its role, the mechanism Gram-positive bacteria employ to secrete virulence factors during infection can be understood. Pathogenic bacteria secrete these virulent proteins to establish an infection, and without the secretion of properly folded and fully functional factors, the chances of establishing virulence are reduced⁴. In Gram-positive bacteria, the PrsA proteins most similar to *LmPrsA2* are *B. subtilis* PrsA and *S. pneumoniae* (*Sp*) PrsA, sharing 68% and 60% similarity, respectively⁶⁴. *B. subtilis* has been characterized for its ability to fold secreted proteins^{69,70} however *B. subtilis* is not a pathogen, making *SpPrsA* a better homolog to study⁶³. *LmPrsA2* varies from the *SpPrsA* sequence across the parvulin and foldase domains, especially at the signature PPIase motif. Although the PrsAs in *Lm* and *Sp* are not well conserved, the function of PrsAs seems to be conserved, where *SpPrsA* insertion into *Lm* is able to retain swimming motility, bacterial resistance to acidic and basic pH, and hemolytic activity⁶⁴. Other functions such as resistance to osmotic shock, antibiotic resistance, and colonization have a significant decrease when *SpPrsA* is substituted for *LmPrsA2*, making it difficult to pinpoint which regions of the proteins may be important for certain functions⁶⁴.

Virulence factors that are secreted from the Sec translocation system are secreted from the cytosol in an unfolded state and must rapidly fold between the bacterial membrane - cell wall interface to become functional^{32,33,71} (Figure 5). Once *LmPrsA2* and *SpPrsA* are secreted and properly folded, they form a covalent bond to lipids within the bacterial membrane and this covalent bond acts as an anchor for the protein^{46,60}. The unfolded proteins can then be transported to either *LmPrsA2* or *SpPrsA* where they can be stabilized before being released into the cell wall or outside of the bacterial cell (Figure 5).

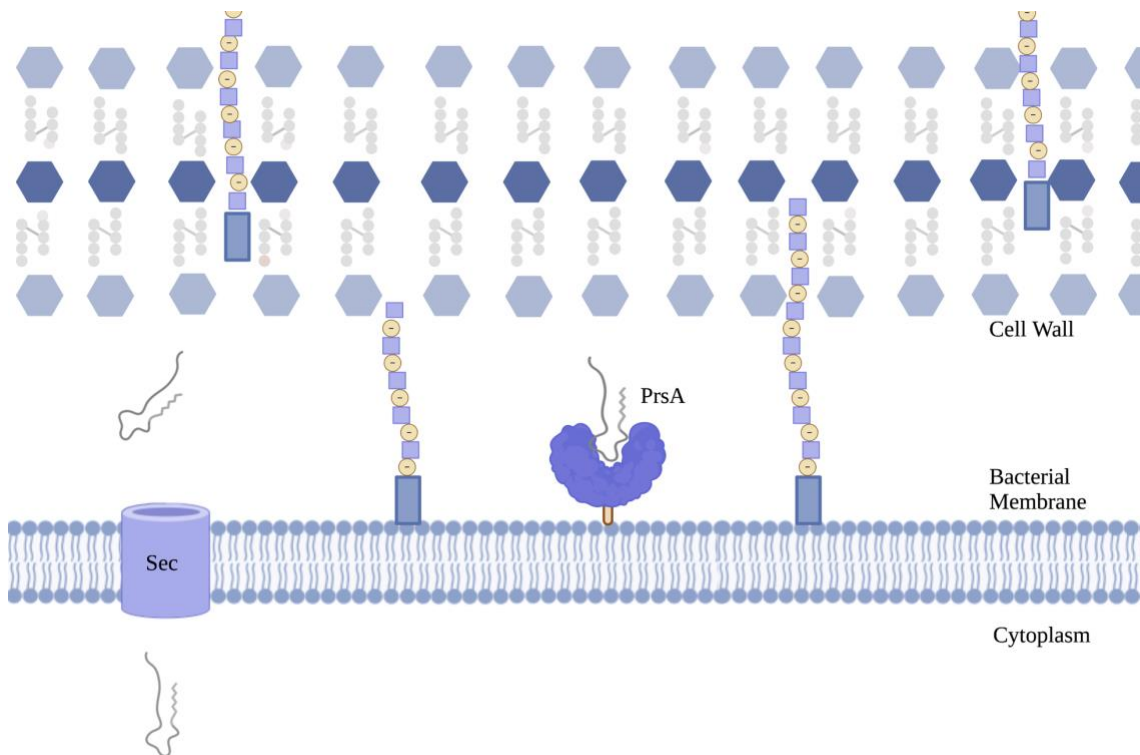


Figure 5. Schematic of post-translocational protein folding in *Lm* and *Sp*.

Unfolded proteins that are secreted from the Sec translocon transit to lipidated PrsA proteins so they can be fully folded before being released into the cell wall or extracellular environment. Image made in

Biorender.

2.1 PORE-FORMING TOXINS AND GRAM-POSITIVE BACTERIAL PRSAS

A major secreted virulence factor in several Gram-positive bacteria includes the cholesterol dependent cytolysins (CDCs), that cause eukaryotic cell lysis by the formation of large pores in cholesterol-containing membranes^{30,57}. In *Lm*, the CDC listeriolysin O (LLO) aids *Lm* in efficiently escaping host cell immune responses by binding to cholesterol in the host vacuole membrane to form a pore for *Lm* to escape and evade an immune response⁸. In a hemolytic assay, which in this instance measures the ability of LLO to lyse red blood cells, we saw that a deletion of the *LmPrsA2* gene led to a defect in hemolytic activity and provided the first link between *LmPrsA2* and LLO^{47,60,72}. So far, we see a similar phenotype in *Sp* with *PrsA* and *Sp*'s pore-forming toxin called pneumolysin (Ply) which is important for disease causation as *ply* deletion mutants showed a significant decrease in virulence in murine models^{63,66}. In a deletion of *SpPrsA*, there is a reduction of hemolytic activity, which heavily implies that the presence of *SpPrsA* can somehow affect Ply activity (Cahoon, unpublished). From data established in *Sp* and *Lm*, we can deduce that *LmPrsA2* and *SpPrsA* regulate fully functional LLO and Ply, respectively, but it is still unclear whether 1. this interaction is direct and 2. if interactions with other virulent proteins with *PrsAs* is possible.

2.1.1 IDENTIFICATION OF LLO AND PLY WITH *LMPRSA2* AND *SPPRSA*

Since there is a reduction in hemolytic activity in *Sp prsA* and *Lm prsA2* deletion mutants, we questioned whether there is a direct interaction between *LmPrsA2* and *SpPrsA* with LLO and Ply, respectively. After the expression and purification of N-terminally labeled 6x His tagged *LmPrsA2*, *SpPrsA*, LLO and Ply proteins, I tested for a direct interaction between the *PrsAs* and

their corresponding pore-forming toxin using two biophysical techniques, Microscale Thermophoresis (MST) and affinity Isothermal Titration Calorimetry (ITC). For MST experiments, we labeled purified *LmPrsA2* and *SpPrsA* with an amine reactive fluorophore (N-hydroxysuccinimide, NHS dye) and utilized these fluorescently labeled proteins to detect an interaction with LLO and Ply. Our results for the interactions of both *LmPrsA2*-NHS with LLO and *SpPrsA*-NHS with Ply indicate that PrsA2-NHS and PrsA-NHS bind to LLO and Ply with physiologically relevant binding affinities (K_D) of 1.3 μM and 85.4 nM, respectively (Figure 6A, 6B).

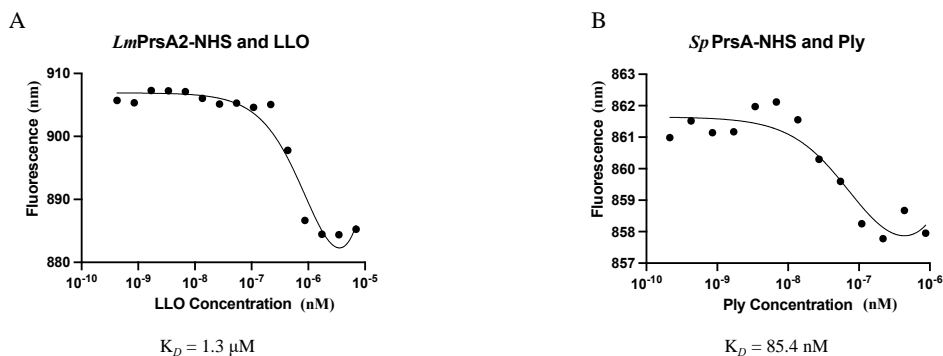


Figure 6. MST of *LmPrsA2* and *SpPrsA* with LLO and Ply

A) MST of *LmPrsA2* with -NHS fluorophore with an increasing concentration of LLO. Two replicates were performed. B) MST of *SpPrsA* with -NHS fluorophore with an increasing concentration of Ply. One replicate was performed.

Using the same labeling strategy, we labeled LLO and Ply with a -NHS tag and performed the reverse experiment (data not shown). Under both conditions, binding was detected for both *LmPrsA2* and *SpPrsA* to LLO and Ply, respectively. To confirm the binding of the PrsA proteins to the pore-forming toxins without the use of fluorophores, which can potentially interfere with the interaction, we used affinity ITC with native, unlabeled purified proteins. As LLO is slowly titrated into a cell containing *LmPrsA2*, the changes in raw heat of the system yields a K_D 567 nM.

The parallel experiment with Ply and *SpPrsA* yields a K_D 82.6 nM (Figure 7). Both ITC and MST results demonstrate the interaction of Ply with *SpPrsA* and *LmPrsA2* with LLO. We see that the molar ratio for *SpPrsA* to Ply is 4:1, indicating that each PrsA tetramer interacts with a Ply monomer. The molar ratio for *LmPrsA2* to LLO was 2:1, indicating that a PrsA2 dimer interacts with one LLO monomer. Taken together, the data obtained suggests that LLO is a client of *LmPrsA2*, and Ply is a client of *SpPrsA*.

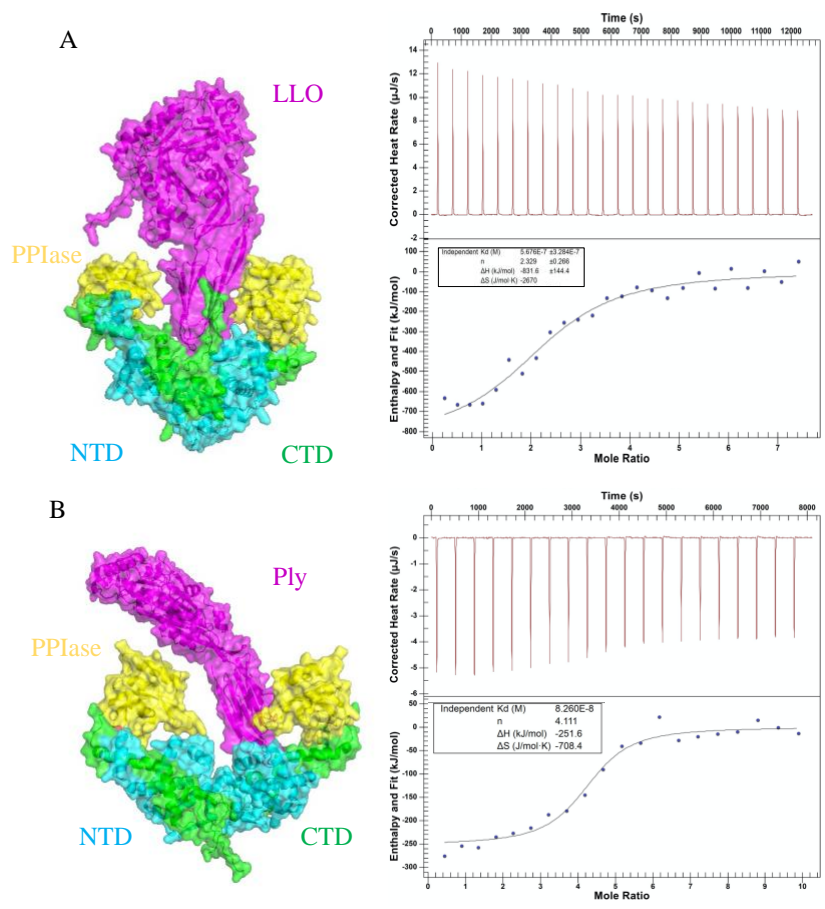


Figure 7. PrsA proteins with pore-forming cytolysins

A) *LmPrsA2* and LLO predicted complex using ColabFold (Mirdita *et al.* 2022) and Affinity ITC results of their binding interaction. An independent fit was used to analyze the data. LLO is depicted in magenta, PPIase in yellow, CTD in green and the NTD in cyan. B) *SpPrsA* and Ply predicted complex using ColabFold (Mirdita *et al.* 2022) and Affinity ITC results of their binding interaction. An independent fit was used to analyze the data. Ply is depicted in magenta, PPIase in yellow, CTD in green and the NTD in cyan.

2.2 IDENTIFICATION OF VARIOUS INTERACTING PARTNERS OF *LmPrsA2* AND *SPrsA*

To investigate other potential interacting partners of *LmPrsA2* and *SPrsA*, a stable isotope labeling of amino acids in cell culture (SILAC) pulldown was performed. *LmPrsA2* pulled down 105 proteins while *SPrsA* pulled down 112 potential interactors. Of the proteins pulled down in *Lm*, only 9 are classified as virulence factors, while in *SPrsA*, only 7 are known are virulence factors. Of the virulence factors identified in the pulldown, I selected InlC and ActA from the *LmPrsA2* pulldown and PBP2B and NanA from the *SPrsA* pulldown to investigate potential roles for the interaction.

In *Lm*, Internalin C (InlC) and actin-assembly inducing protein A (ActA) act as major constituents of bacterial virulence. The internalin protein family is critical in *Lm* virulence as it helps form protrusions in the host cell plasma membrane to allow the bacteria to enter and exit neighboring cells to continue the course of the infection⁷³. Although the family of internalin proteins act as virulence proteins, only InlB and InlC appeared on the SILAC pulldown as interacting with *LmPrsA2* with a high association. After performing ColabFold⁷⁴ on *LmPrsA2* with inlB and inlC, there seems to be no predicted interaction between inlB and *LmPrsA2*, indicating that the SILAC pulldown interaction may be indirect (data not shown). However, *LmPrsA2* is predicted to interact with InlC (Figure 8). InlC's specific role is to assist in protrusion formation by disrupting the tension of host actin in the plasma membrane so that *Lm* can exit the cell⁷⁵⁻⁷⁷. ActA is a critical virulence factor in *Lm* because it's responsible for actin polymerization for formation of an actin comet tail to promote *Lm*'s ability to transit in the host while infecting it⁸. The first link between *LmPrsA2* and ActA was discovered when a *prsA2* deletion caused a significant defect in *Lm* motility^{59,64}. Further support is shown from the SILAC pulldown data

where *LmPrsA2* pulled down ActA, suggesting an interaction between the two proteins. They are predicted to interact via ColabFold⁷⁴ where we suspect it may interact with *LmPrsA2*'s PPIase domain shown in yellow (Figure 8).

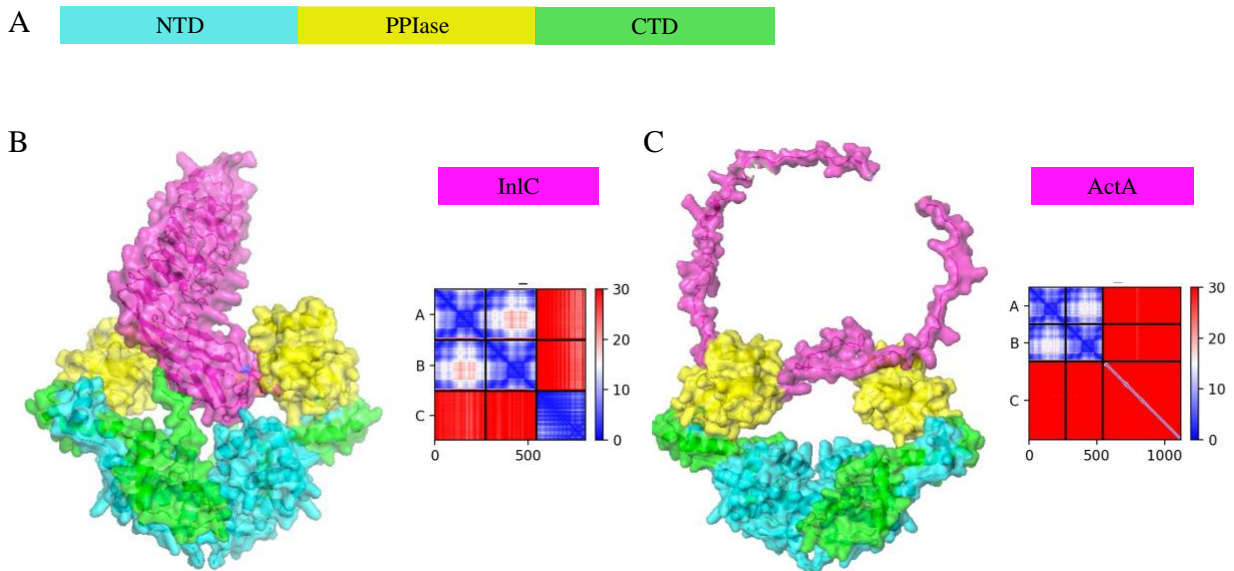


Figure 8. ColabFold Structure of *LmPrsA2* with InIC and ActA.

A) Schematic of PrsA2 domains B) InC-PrsA2 complex with domains of PrsA2 colored as described in A and InIC shown in magenta. Predicted align error show to right. C) ActA-PrsA2 complex with domains of PrsA2 colored as described in A and ActA shown in magenta. Predicted align error show to right.

The potential for *LmPrsA2* to interact with many virulence factors suggests that this may be true for other PrsAs in pathogenic Gram-positive bacteria. In *Sp*, I chose to investigate neuraminidase A (NanA) and PBP2b, two proteins identified in the SILAC pulldown that act are major components of *Sp* virulence^{6,78}. In an assay developed to measure the ability of the NanA to cleave sialic acids off carbohydrates in host mucus *in vivo*, there is a reduction in the ability to cleave these acids when NanA is deleted⁷⁹. One function of pneumococcal neuraminidases is to help *Sp* evade an immune response by cleaving host immune defense proteins⁷⁸. While no direct

evidence has been established linking the function of *SpPrsA* with NanA, ColabFold⁷⁴ predicts that these proteins interact (Figure 9). The next protein family of interest identified in the SILAC pulldown are penicillin-binding proteins (PBPs) which are essential components of the Gram-positive cell wall that provide protection from external stressors and antibiotics⁸⁰. In addition to being identified as a potential interactor in the SILAC pulldown, PBP2b is destabilized in a *prsA* deletion in *B. subtilis* suggesting that PrsA is responsible for folding it⁵⁸, which provided the first link between PrsA and PBP2b. *SpPrsA* and PBP2b are predicted to interact via ColabFold structure and SILAC pulldown (Figure 9).

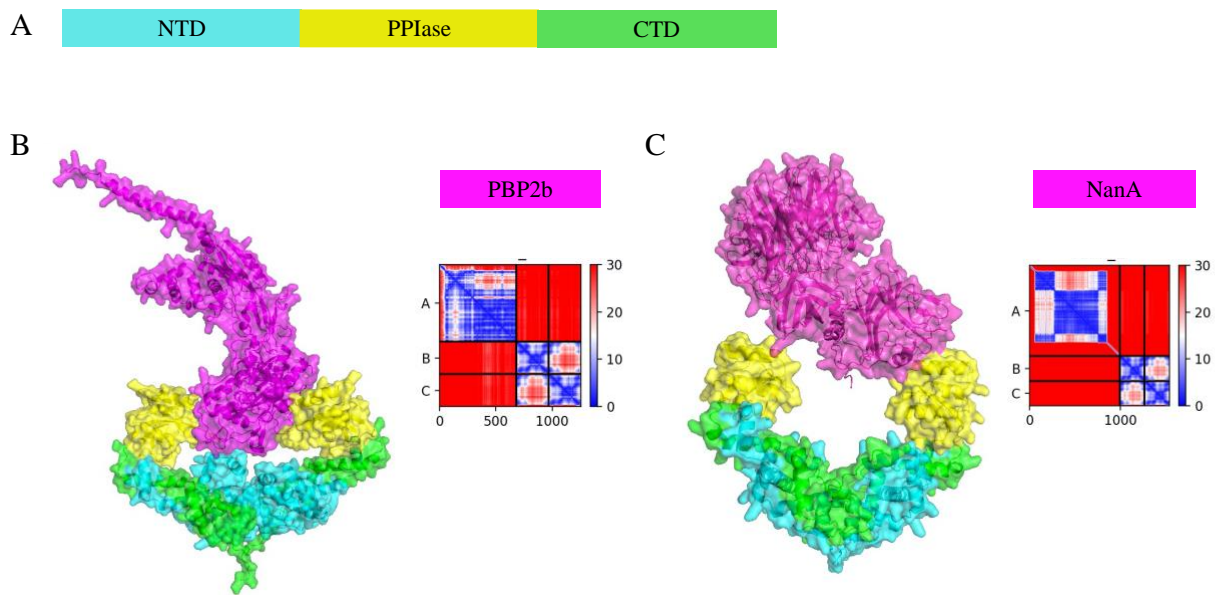


Figure 9. ColabFold Structure of *SpPrsA* with PBP2B and NanA.

A) Schematic of PrsA domains B) PBP2b-PrsA2 complex with domains of PrsA colored as described in A and PBP2b shown in magenta. Predicted align error show to right. C) NanA-PrsA complex with domains of PrsA colored as described in A and NanA shown in magenta. Predicted align error show to right.

2.2.1 COLABFOLD AS A METHOD TO IDENTIFY PROTEIN-PROTEIN INTERACTIONS

For prediction of protein-protein complexes, we used ColabFold⁷⁴, which is an accessible, cloud-based implementation of AlphaFold²⁸¹, a deep-learning based protein structure prediction method that can accurately predict the secondary structure and tertiary arrangements of highly structured proteins. ColabFold offers more user-tunable parameters than AlphaFold and uses mmseqs2⁸² as an MSA generator. Specifically, since we are looking at protein complexes, we used AlphaFold-multimer⁸³. Using this method, I was able to predict the interactions of *LmPrsA2* and *SpPrsA* with the potential interacting proteins from a SILAC pulldown assay. Disordered regions with long, unstructured regions have high margins of error in structural predictions; therefore, I omitted those regions from ActA and InlC and instead included the functional domains (Figure 8, 9). Of special interest is the interaction between ActA's proline rich repeat region and *LmPrsA2* due to this area being a target for PPIases, motivating me to delete the disordered regions and focus on the interactions with *LmPrsA2* (Figure 8). Similarly, only NanA's functional domains, the lectin-like and neuraminidase domains, were inputted into ColabFold with *SpPrsA* compared to full-length NanA. In both scenarios, the functional domains are predicted to interact with *SpPrsA*. The ability of ColabFold to accurately predict the tertiary structures of the proteins in a complex depends on factors, such as known structures of similar proteins or presence of disordered regions, and the corresponding predicted align error diagrams show a high confidence to predict PrsA, while highly unstructured proteins such as ActA and NanA have less certainty.

2.3 DISCUSSION

Using MST and ITC, we show that *LmPrsA2* and *SpPrsA* have high affinity interactions with LLO and Ply, respectively. Interestingly, hydrophobic residues of both LLO and Ply are seen in the hydrophobic pockets of *LmPrsA2* and *SpPrsA*, respectively. Using ColabFold⁷⁴ we also predict *LmPrsA2* and *SpPrsA* to interact directly with virulence factors, InlC, ActA, NanA and PBP2b. To complement the ColabFold data, those virulence factors were pulled down with either *LmPrsA2* or *SpPrsA* *in vivo* using secreted bacterial supernatants in a SILAC pulldown. InlC seems to fit nicely into the hydrophobic pocket of *LmPrsA2* and is near both the PPIase and foldase domains of *LmPrsA2*. Because the predictions suggest interactions of ActA with the PPIase domain of *LmPrsA2*, I included only the proline-rich repeat region of ActA (Figure 8) while deleting the rest of the sequence. When the entire sequence of ActA is input into ColabFold, we see association solely between *LmPrsA2* and the proline-rich regions of ActA (not shown). The protein complex formed by *LmPrsA2* and ActA exhibit ActA's proline-rich region being 'fed' directly through the PPIase domain. Overall, the interactions with ActA and InlC in both our pulldown and structural predictions suggests direct interactions with *LmPrsA2*, where the PPIase domain could be catalyzing *cis-trans* conformations of residues N-terminal to proline.

Similarly to ActA and *LmPrsA2*, the functional domains of NanA, and not the disordered linking regions, were used to detect a potential interaction between NanA and *SpPrsA*. When compared to the full-length NanA, we see no interaction between these domain-linking regions of NanA and *SpPrsA* in all 5 models from ColabFold. Based on evidence of interaction between NanA and *SpPrsA* from the SILAC pulldown and the ColabFold predicted complex, I suspect that *SpPrsA* may directly interact with NanA directly through the PPIase domain, as the PPIase domain may be catalyzing NanA. Furthermore, in methicillin-resistant *S. aureus* (MRSA), an extra PBP is

expressed that allows it to have a low affinity for certain antibiotics and although this additional PBP allows for antibiotic evasion, the presence of function this PBP is dependent on the PrsA activity⁸⁴. In *Sp*, PrsA interacts with PBP2b via the SILAC pulldown, and though it is unclear whether this is an indirect or direct interaction, the potential for them to interact is likely. The PBP2b is interacting with both domains of *Sp*PrsA and is deep within the hydrophobic pocket. Overall, the exact reasoning why these virulence factors interact is unclear, but there is evidence to support direct interactions. Direct interactions between InlC, ActA, NanA, and PBP2b with *Lm*PrsA2 or *Sp*PrsA are predicted because PrsAs may fold and/or stabilize these virulence factors.

2.4 FUTURE DIRECTIONS

The successful confirmation of high affinity interactions between *Lm*PrsA2 and *Sp*PrsA with LLO and Ply, respectively, highlights the possibility of strong interactions between *Lm*PrsA2 and *Sp*PrsA with the remaining virulent proteins identified in the SILAC pulldown. The next steps of this project will be to define interactions between *Lm*PrsA2 or *Sp*PrsA and the virulence factors within *Lm* and *Sp*. In these Gram-positive bacteria, the virulence proteins necessary for establishing infection seem to have a common denominator: they are predicted to interact with PrsA. ColabFold predicted protein complexes with PrsAs and inlC, ActA, PBP2b, or NanA. My goal is to determine if, like LLO and Ply, *Lm*PrsA2 and *Sp*PrsA directly bind to these virulence factors using Affinity ITC. I anticipate there to be direct interactions between these proteins, but if there is no binding detected I plan to investigate how the proteins relate during virulence. Upon

confirmation of a direct interaction, I would then determine if *LmPrsA2* and *SpPrsA* knockouts lead to a defect in function similar to deletions in the *InlC*, *ActA*, *PBP2b* and *NanA* genes.

Further experimentation will include surveying protein secretion levels of the virulence factors and in the wildtype and *PrsA* deletion mutants. Decreased or increased levels will suggest further roles of *PrsA* proteins in protein regulation. These proposed experiments would uncover if *LmPrsA2* and *SpPrsA* directly influence *InlC*-mediated protrusion formation, *ActA* actin polymerization, *PBP2b* peptidoglycan fortification or *NanA*-dependent sialic acid cleavage. Understanding the relationship between *PrsAs* and these proteins in virulence will help us to target these mechanisms using antivirulence based therapeutics.

3.0 IDENTIFYING THE ACTIVE DOMAINS WITHIN PRSA PROTEINS

3.0 INTRODUCTION

PrsA proteins' pivotal role in Gram-positive pathogenic virulence suggests that inhibiting it could increase the chances of bacterial clearance, even for immunocompromised individuals who are not responding to antibiotics. Parvulins offer a potential avenue for the treatment of pathogenic bacteria⁵⁵, but difficulties arise in the search of a model inhibitor. Current research investigating parvulin inhibitors has not developed far past the use of juglone, an inhibitor of Pin1 that has not been able to meet the criteria of a successful drug: stability, cell permeability, potency, and selectivity^{54,55}. To find a druggable target in *LmPrsA2* and *SpPrsA*, we must identify and subsequently inhibit the regions of either the foldase and/or the PPIase domain that interact with other biomolecules. Our current understanding of the PPIase and foldase domains is lacking, as some PrsAs are not predicted to have PPIase activity but have overlapping functions with PPIase active PrsAs⁶⁴. The goals of my project are to establish which region(s) of *LmPrsA2* and *SpPrsA* are critical recognition and binding with other proteins and to unveil which functional regions within PrsAs could be targets for inhibition.

3.0.1 THE PPIASE AND FOLDASE DOMAINS

It's predicted that streptococcal species with PrsA proteins also lack PPIase activity based on a missing signature PPIase motif important for prolyl isomerization: F-[GSADEI]-x-[LVAQ]-A-x(3)-[ST]-x(3,4)-[STQ]-x(3,5)-[GER]-G-x-[LIVM]-[GS], which *S. pyogenes* PrsA1 and PrsA2,

SpPrsA, and *S. mutans* PrsA lack^{64,85,86}. Although each of these streptococcal signature PPIase motifs in PrsA homologs differ by only 2-5 residues from PrsA in *L. monocytogenes* and *B. subtilis*, they cannot catalyze the *cis*-to-*trans* isomerization of residues N-terminal to proline in the substrates they fold likely due to the changes in overall charge or polarity of that region^{59,64,87,88}. The foldase domain of PrsAs is made up of an N-terminal domain and C-terminal domain. While some PrsAs have been measured for their PPIase activity, none have been measured specifically for their foldase domain activity. For example, the Gram-negative bacteria *E. coli* contains a parvulin protein named SurA, which has been extensively researched. While the protein is capable of folding extracellular proteins, this folding has not been linked specifically to the PPIase and/or the foldase domain⁸⁹.

3.0.2 OVERLAPS IN FUNCTIONS OF PRSAS

Some Gram-positive bacteria have more than one PrsA homolog, such as PrsA1 and PrsA2 within *L. monocytogenes* and *S. pyogenes*. Deletion of the *L. monocytogenes* *prsA2* results in several virulence defects while *L. monocytogenes* PrsA1 contributes to bacterial translocation across the intestinal wall⁹⁰⁻⁹². Both *LmPrsA1* and *LmPrsA2* demonstrate PPIase activity, however PrsA1 appears to have a supporting role to PrsA2 during intragastric infection and PrsA1 is dispensable in the septicemic model of infection^{91,93}. When the NTD of *LmPrsA2* is swapped for the NTD of *LmPrsA1*, there is less hemolytic activity and growth, but when the PPIase domain are swapped there is no defect in either assay, indicating the NTD domain of *LmPrsA2* is important for protein recognition⁵⁹. In *S. pyogenes*, the two homologs of PrsA (*SpyPrsA1* and *SpyPrsA2*) individually contribute to secreted protein homeostasis and share overlapping function in host adherence,

biofilm formation and virulence in a murine mouse model⁸⁶. But unlike *LmPrsA1* and *LmPrsA2*, *SpPrsA1* and *SpPrsA2* do not contain the signature PPIase motif and are not predicted to have PPIase activity^{86,92}.

3.1 IDENTIFICATION OF FUNCTIONAL REGIONS OF *LMPRSA2* AND *SPPRSA*

Current literature suggests the PPIase domain of *LmPrsA2* is dispensable for hemolytic activity in *Lm*, where a deletion of the PPIase domain displays levels comparable to wild-type *LmPrsA2*⁵⁹. Using ITC, I have found that a *LmPrsA2* N+C mutant, with a deletion of the entire PPIase domain, binds to LLO with $K_D = 109.7$ nM (Figure 10) which has a higher affinity than WT *LmPrsA2*'s affinity to LLO (Figure 7). Similarly, a deletion of the PPIase domain in *SpPrsA* results in a slight defect in binding to Ply, yielding a $K_D = 1.86$ μ M, which is much higher than wild-type *SpPrsA*'s affinity to Ply (Figure 7). Because the interactions between the two proteins still occur, my preliminary data and literature suggest the PPIase domains of *LmPrsA2* and *SpPrsA* are not necessary for protein recognition. To determine which regions of *LmPrsA2* interact with LLO more efficiently than randomized mutagenesis, I used ColabFold to predict the structure of the *LmPrsA2* N+C mutant with LLO⁶⁰ (Figure 11). From the predicted interaction, we can see the C-terminal Domain (CTD) of LLO is in the inner pocket formed by the *LmPrsA2* foldase dimer. This region is highly hydrophobic, with the potential for favorable pi stacking interactions between the aromatic side chains present in this potential binding region. There is no overall charge of this binding pocket from either *LmPrsA2* or LLO, highlighting the importance of hydrophobicity, and not electrostaticity, in the interaction.

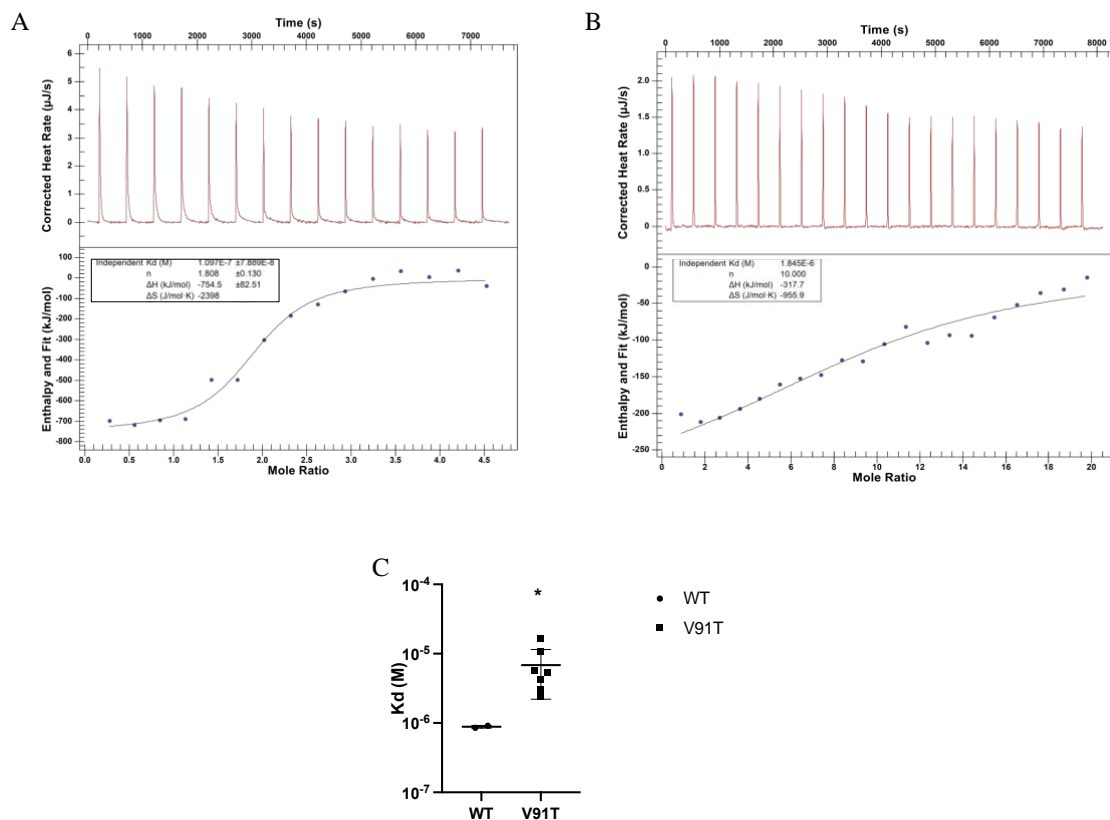


Figure 10. PrsA N+C Mutants with LLO and Ply

A) Affinity ITC data of the *LmPrsA2* N+C deletion mutant with LLO exhibiting a high affinity.

B) Affinity ITC data of the *SpPrsA* N+C deletion with Ply exhibiting a binding interaction. C) V91T Mutant data

of *LmPrsA2* shows a significant defect to bind to LLO. N = 7 independent experiments of the V91T data, N=2 of

WT. A two-tailed, unpaired t-test was performed to derive statistical significance with a p value < 0.05

Furthermore, a V91T mutation has been shown to reduce hemolytic activity suggesting a role for this residue in the interaction with LLO⁵⁸. I labeled purified V91T with a NHS fluorophore and, using MST with LLO, observed a significant decrease in the affinity of *LmPrsA2* V91T to LLO with a $K_D = 1.14 \mu\text{M}$ (Figure 10C), compared to WT with a $K_D = 567 \text{ nM}$ (Figure 7). The affinity decreased by three-fold, suggesting this amino acid may be critical for the interaction with LLO. To further investigate potential mutants within the foldase domain that can contribute to a

decreased affinity for binding partners, I used the ColabFold model to identify residues that could be interacting with the PPIase deletion mutant (Figure 11). Two residues in the foldase domain within close proximity to LLO (magenta) are V112 and T251. V112 in the NTD could be having some hydrophobic interactions with tyrosine in LLO, while T251 in the CTD is interacting with

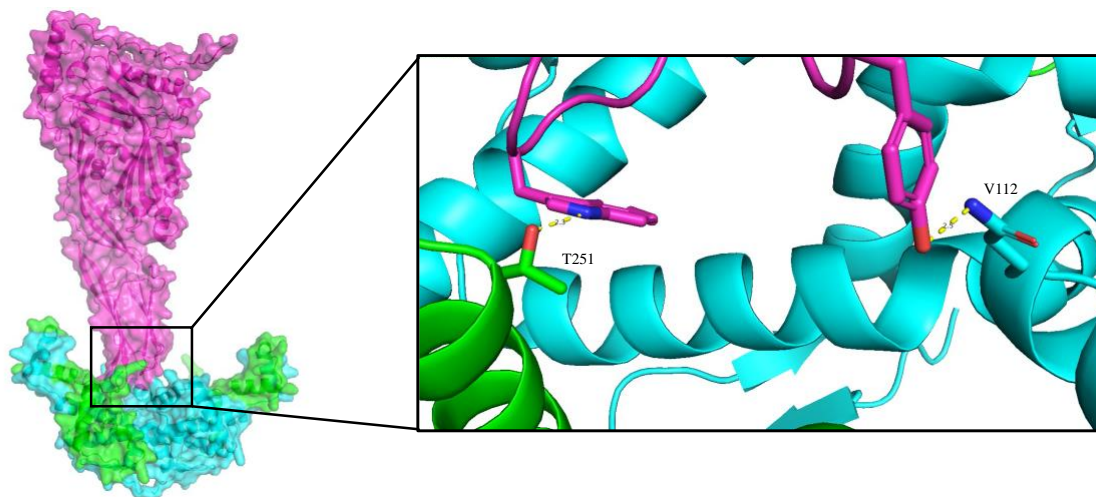


Figure 11. *LmPrsA2* N+C Mutant with LLO

ColabFold predicted interaction between a PPIase deletion mutant of *LmPrsA2* with LLO. The region of close proximity between the two is emphasized on the right, highlighting the potentially critical residues PrsA2 in the CTD (green) and NTD (cyan) with LLO (magenta).

tryptophan in LLO and can have polar interactions. The bond length between the oxygen and nitrogen atoms denoted in Figure 11 in the valine-tyrosine interaction are about 2.3 Å apart and are most like forming hydrogen bonds. The bonds forming between tryptophan and threonine have a bond length over about 2.5 Å indicating that hydrogen bonds can be occurring here as well.

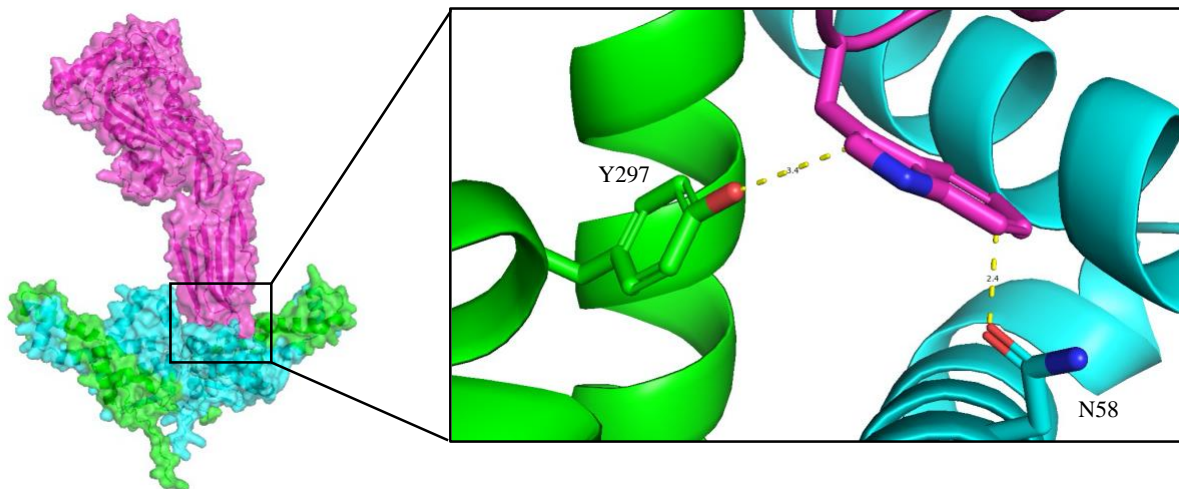


Figure 12. Colab Structure of *SpPrsA* N+C Mutant with Ply

ColabFold predicted interaction between a PPIase deletion mutant of PrsA2 with LLO. The region of close proximity between the two is emphasized on the right, highlighting the potentially critical residues PrsA2 in the CTD (green) and NTD (cyan) with LLO (magenta).

From the preliminary ITC data, the N+C mutant of *SpPrsA* bound to Ply with an affinity of 1.85 μM which is comparable to WT. Although no preliminary mutagenesis was performed for *SpPrsA* foldase mutants, I performed ColabFold of the N+C mutant with Ply (Figure 12). Hydrophobic interactions and hydrogen bonding seem to be responsible for the interaction between Ply and PrsA, with tryptophan of Ply potentially forming bonds with Y297 of the CTD of *SpPrsA* and N98 of the NTD of *SpPrsA*.

3.2 PRSA AS A THERAPEUTIC TARGET

The ChEMBL drug bank has compiled 2.2 million compounds globally into an accessible repository for potential therapeutics. Using this knowledge, I first narrowed down the list of potential *LmPrsA2* inhibitors from the 2.2 million total drugs to about 1,920,338 targets by solely selecting for small molecules. Although there is debate between the use of small molecules vs peptides, and peptides show to be more specific, they have poor pharmacokinetic scores *in vivo*^{63,64} leading me to opt for a small molecule inhibitor. I further subdivided the results to exclude drugs that were not specific for bacteria, and then excluded Gram-negative specific compounds in the database. This filtering process now leaves 744 compounds left for testing. After applying a filter that excludes chemicals that violate the Lipinski rule of five, which measures the likeliness of a compound to be an effective, orally available drug⁹⁴, the list narrowed down to 135 eligible compounds (Figure 13). Once more data is obtained about residues critical for binding, I will be able to narrow down the number of results to select for a more specific target of the *LmPrsA2* and *SpPrsA* binding pocket.

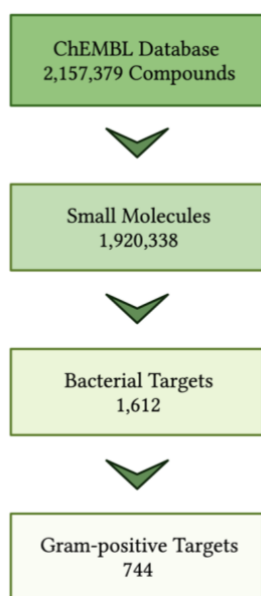


Figure 13. Targeting PrsA Inhibition

Small molecule inhibitors from data based narrowed down based on Lipinski rule of five.

3.3 DISCUSSION

Parvulins can catalyze *cis-trans* isomerization but during a divergence in evolution, some PrsAs encoded in Gram-positive genomes lost their ability to utilize their PPIase activity. PPIase activity dispensability can partially be attributed to foldase domain activity, which is a common trait among molecular chaperones, that allow proteins to be folded, unfolded and/or refolded before they are released²⁶ if the foldase domain plays a larger role than the PPIase domain. Both *LmPrsA2* and *SpPrsA* seem to be responsible for fully folding proteins, as suggested in hemolytic assays measuring the ability of LLO and Ply to function⁵⁹ (Cahoon unpublished), or somehow participating in a mechanism that allows these proteins become fully functional. Although there are important implications for PrsAs in these organisms, the deletion of the PPIase domain in *LmPrsA2* led to a significant decrease in virulence in a mouse model⁵⁹. Whether this is due to a diminished ability to ‘grab’ onto interacting proteins or to contribute to the overall stability of the protein is unclear.

As far as critical residues required for foldase activity, we see potential with V112 in *LmPrsA2*'s NTD and T251 in its CTD. As for *SpPrsA*, N58 in the NTD and Y297 in the CTD are suggested to be important for the interaction from the ColabFold prediction. When WT *LmPrsA2* is bound to LLO, foldase residues Y84 and Q94 are seen 0.8 Å and 1.9 Å apart from LLO, respectively, from Trp of LLO in the binding pocket (Figure 11). In the predicted interaction of *SpPrsA* and Ply, only foldase residue Q112 showed close interactions with Ply, with a bond distance of 1.9 Å. In total, the bond lengths suggest hydrophobic interactions or hydrogen bonding are at play, which support our theory of PrsA's being involved in transient interactions. Stronger bonds, such as covalent bonds, may be harder to break than hydrogen bonds during the protein folding process.

3.4 FUTURE DIRECTIONS

The next step of this project is to narrow down the list of potential small molecules from the ChEMBL drug database by visualizing the *Lm* PrsA2/LLO and *Sp*PrsA/Ply interactions using MD simulations. The simulations will reveal the structural changes *Lm*PrsA2 and *Sp*PrsA undergo while binding a protein which is information that we cannot achieve from a static image on ColabFold. For example, *Lm*PrsA2 could undergo a structural rearrangement when bound to LLO and reveal binding regions not seen in an unbound model. Thus far, we see potential of the hydrophobic pocket in both PrsAs for protein binding. If the MD simulations also reveal this region to be important for protein recognition, we can confirm *in vitro* by mutating this pocket to disrupt its hydrophobicity by mutating residues that have a positive charge and see if this change hinders the ability of LLO or Ply to bind. In terms of an inhibitor, we know the K_D of LLO to *Lm*PrsA2 is 567 nM so the association of the compound to *Lm*PrsA2 must be much tighter to ensure it can outcompete LLO and other *Lm* proteins. Additionally, the MD simulations will help us narrow down the 744 potential small molecule inhibitors in Figure 13 by allowing us to exclude small molecules with charges, polarity, etc. that would not bind to these important regions. Instead of looking at ligands bound to a static model, the simulations will show if these drugs can bind to the target in *in vivo* like conditions, where the target is fluctuating in conformations. For example, certain conditions may cause *Lm*PrsA2 to bury surface residues within the protein that will only be revealed upon binding to a protein.

Next, I would utilize docking to test the narrowed down compounds directly on *Lm*PrsA because it can predict which inhibitors are able to bind to the target, allowing us to exclude compounds that show unfavorable interactions before testing each inhibitor individually *in vitro* or *in vivo*. Upon narrowing down the search for a small molecular inhibitor, I would then test these

drug candidates as to whether they can bind to *LmPrsA2* using MST, which is an ideal method for binding assessments for drug discovery⁹⁵⁻⁹⁹. I will determine the ability of the candidate drugs to bind *LmPrsA2*-NHS with the goal of finding a small molecule that has a higher binding affinity to *LmPrsA2* than *LmPrsA2*'s affinity to the virulence factors because the compounds need to outcompete native proteins in *Lm*. These proposed experiments will help to find a suitable inhibitor of *LmPrsA2* that can potentially be used to inhibit *SpPrsA* and other PrsA proteins in pathogenic bacteria.

4.0 MATERIALS AND METHODS

4.0 PROTEIN PURIFICATION

S. pneumoniae PrsA

Genomic DNA from *S. pneumoniae* strain 19A was used to amplify *prsA* (ZP_06978074.1; residues 27 to 313) which was cloned into the pMCSG53 expression vector containing an N-terminal His6x-tag followed by a TEV protease cleavage site, encoding ampicillin resistance, and genes for rare codons. PrsA was expressed in *E. coli* BL21(DE3) Gold cells, grown to an OD600 of 0.6 at 37 °C, chilled to 16 °C, and induced overnight with 500 µM IPTG. Cells were harvested via centrifugation at 5000 × g, pellets were resuspended in binding buffer (50 mM HEPES (pH 7.5), 300 mM sodium chloride, 10 mM imidazole, and 2% glycerol (v/v)) and lysed by sonication, and cell debris was removed via centrifugation at 30000 × g. Cleared lysate was loaded onto a 5 mL Ni-NTA column (QIAGEN) pre-equilibrated with binding buffer and extensively washed with binding buffer containing 30 mM imidazole, and protein was eluted using the above buffer supplemented with 250 mM imidazole. Then the protein was dialyzed at 4°C overnight in dialysis buffer (20mM MES, 100mM NaCl, 1mM beta-mercaptoethanol, 10% glycerol). Protein concentration was measured by BCA assay (Pierce).

S. pneumoniae Ply

Genomic DNA from *S. pneumoniae* strain TIGR4 was used to PCR amplify the open reading frame of *ply* which was cloned into the pQE30 expression vector (Qiagen) containing an N-terminal His6x-tag. Positive clones were selected on LB agar plates containing 50 µg/ml carbenicillin and

confirmed by DNA sequencing analysis. Ply was expressed in *E. coli* BL21(DE3) Star cells where a single colony was picked from LB agar plates containing 50ug/ml carbenicillin and inoculated into 10 mL of LB broth supplemented with 50 µg/mL of carbenicillin with shaking at 37° C for 16 hours. Then 5mL of the 16-hour culture was used to inoculate 1L LB broth containing 50 µg/mL of carbenicillin. Culture was grown until OD₆₀₀ = 0.6 and IPTG was added to a final concentration of 0.8mM to express the recombinant Ply protein. The culture was grown with shaking at 30°C for 12 hours and centrifuged and pelleted cells were flash frozen and stored -80°C until further processing. Pelleted cells were thawed and resuspended in chilled wash buffer (50mM Tris pH 7.5; 500mM NaCl; 25mM imidazole) and protease inhibitor cocktail set 3 (Millipore-Sigma) and DNase I (Millipore-Sigma) were added. The cells were lysed by sonication with 10 cycles of 10 seconds pulses. Lysate was centrifuged at 8000 rpm for 40 minutes and the suspension was passed through a Ni-NTA column. The protein was washed and eluted using elution buffer (50mM Tris pH 7.5, 500mM NaCl, 500mM imidazole). Then the protein was dialyzed at 4°C overnight in dialysis buffer (20mM MES, 100mM NaCl, 1mM beta-mercaptoethanol, 10% glycerol). Protein concentration was measured by BCA assay (Pierce).

L. monocytogenes PrsA2

Genomic DNA from *L. monocytogenes* 10403S was used to amplify *prsA2* (residues 22 to 272) which was cloned into the pQE30 expression vector containing a C-terminal His₆x-tag. PrsA2 was expressed in *E. coli* BL21(DE3) Gold cells, grown to an OD₆₀₀ of 0.6 at 37 °C, chilled to 20 °C, and induced overnight with 800 µM IPTG. Cells were harvested via centrifugation at 5000 × g, pellets were resuspended in binding buffer (50 mM HEPES (pH 7.5), 300 mM sodium chloride, 10 mM imidazole, and 10% glycerol (v/v)) and lysed by sonication, and cell debris was removed

via centrifugation at $30000 \times g$. Cleared lysate was loaded onto a 5 mL Ni-NTA column (QIAGEN) pre-equilibrated with binding buffer and extensively washed with binding buffer containing 30 mM imidazole, and protein was eluted using the above buffer supplemented with 250 mM imidazole. Then the protein was dialyzed at 4°C overnight in dialysis buffer (20mM MES, 100mM NaCl, 1mM beta-mercaptoethanol, 10% glycerol). Protein concentration was measured by BCA assay (Pierce).

L. monocytogenes LLO

Genomic DNA from *L. monocytogenes* was used to amplify *hly* (residues 25 to 529) which was cloned into the pQE30 expression vector containing a C-terminal His₆x-tag. LLO was expressed in *E. coli* BL21(DE3) Gold cells, grown to an OD₆₀₀ of 0.6 at 37°C , chilled to 20°C , and induced overnight with 200 μM IPTG. Cells were harvested via centrifugation at $5000 \times g$, pellets were resuspended in binding buffer (50 mM HEPES (pH 7.5), 300 mM sodium chloride, 10 mM imidazole, and 10% glycerol (v/v)) and lysed by sonication, and cell debris was removed via centrifugation at $30000 \times g$. Cleared lysate was loaded onto a 5 mL Ni-NTA column (QIAGEN) pre-equilibrated with binding buffer and extensively washed with binding buffer containing 30 mM imidazole, and protein was eluted using the above buffer supplemented with 250 mM imidazole. Then the protein was dialyzed at 4°C overnight in dialysis buffer (20mM MES, 100mM NaCl, 1mM beta-mercaptoethanol, 10% glycerol). Protein concentration was measured by BCA assay (Pierce).

4.1 MICROSCALE THERMOPHORESIS (MST)

Proteins were labeled with NanoTemper 2nd Generation Red NHS Dye (Nanotemper Technologies), photosensitive samples were incubated for 30 minutes in a dark room, and then passed through a column to remove excess red NHS dye and the flowthrough containing each labeled protein was collected. The degree of label (DOL) was calculated using the formula: $A_{650}/195,000/M/cm \times \text{concentration of labeled protein}$, where A_{650} =Absorbance at 650 and 195000/M/cm is the molar absorbance of the red NHS dye. A DOL value of 0.7-1.0 was considered optimal labeling. The labeled proteins were aliquoted into small volumes, flash frozen, and stored at -80°C for experimental application. To test the binding interaction between two proteins (labeled and unlabeled), a serial dilution using 10 uL of the unlabeled protein was prepared in low binding microfuge tubes and 10uL of labeled protein (20 nM final concentration) was added to each serial dilution. Then 10 μL of each reaction was loaded into capillary tubes (Nanotemper Technologies) and each sample contained 0.05% tween to prevent aggregation. Each tube containing a serial dilution was loaded into capillary tubes and ran in the Monolith MicroScale Thermophoresis (MST) at 20-100% excitation power and 50% MST Power at 25°C. Data were analyzed using Monolith Analysis Software. Standard error of the mean (SEM) of three independent replicates were calculated.

4.2 AFFINITY ISOTHERMAL TITRATION CALORIMETRY (ITC)

Frozen purified protein aliquots were thawed and then degassed for 15 minutes while acclimating to room temperature (25°C). The ITC sample cell was equilibrated three times with 500 μL of

storage buffer (20 mM MES, 100 mM NaCl, 1 mM BME, 10% glycerol, pH of 6.5) sample buffer before protein loading. The loading syringe was equilibrated with 300 μ L storage buffer before protein was loaded. After heat levels were stabilized, 2-5 μ L increments of protein in the syringe was injected into the sample cell in 400 second increments between each injection for a total of 20 times. The raw heat rates were converted to binding enthalpies (kJ/mol) and the heat of dilution from control experiments was used as a correction factor. The independent binding model was used for the non-linear regression curve fit using NanoAnalyze software (TA instruments).

4.3 PROTEIN COMPLEX STRUCTURE PREDICTION

The AlphaFold-multimer-v2 ColabFold implementation of AlphaFold2 was used for all structural predictions without run relax. Each protein sequence along with the appropriate binding partner sequence was used as the input for the protein prediction model. All predictions were made using mmseqs2 for multiple sequence alignment (MSA). MSA was done with paired sequences from the same species and with an unpaired MSA. Each set of sequences was run with a recycle count of 3, which determines the number of times the prediction is repeatedly fed through the model, and the output included 5 predicted structures sorted by ranking. The ranking of each structure and the overall prediction quality was assessed by the following metrics: sequence coverage and diversity; pLDDT (predicted local distance difference test), which is a per-residue confidence metric; the template modeling score (TM-score); and the associated inter-chain predicted alignment error (inter-PAE).

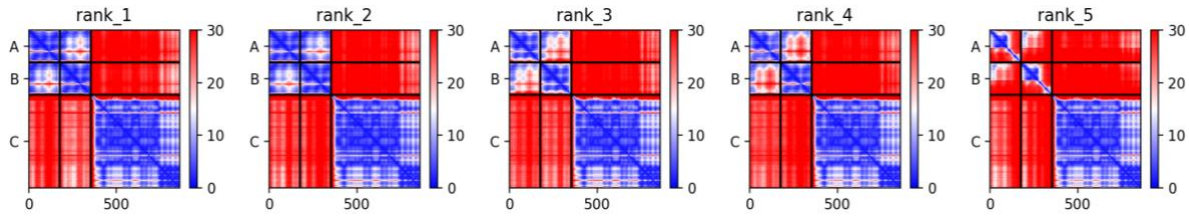


Figure 14 Predicted Alignment Error of Protein Complex

Detected error from the top 5 predicted complexes of the *LmPrsA2* N+C mutant with LLO. Rankings are based on percent error with red corresponding to a higher error, while blue represents less error.

4.4 STABLE ISOTOPE LABELING OF AMINO ACIDS IN CELL CULTURE (SILAC) PULLDOWN

For the SILAC Pulldown, cells were cultured in media containing heavy and light lysine enriched in stable isotopes. Cells were then grown in either heavy or light media incubated with control or bait beads, respectively. Either *LmPrsA2* or *SpPrsA* were used as bait on the bait beads. Beads were washed before being combined and boiled to collect the bound proteins. Proteins were then used to perform sodium dodecyl sulphate–polyacrylamide gel electrophoresis (SDS-PAGE). Proteins were then fractionated, then processed via alkylation and tryptic digestion step by step in the centrifugal unit. After overnight digestion at 37°C, the peptides were eluted twice with 50 µL 0.1% formic acid (FA). The concentration of proteins and peptides collected in each step was measured using a Nanodrop ONE (Thermo Scientific, San Jose, CA). The digested peptides were then desalted, dried, and stored at –80 °C until further use. The samples were dried and resulting pellets stored in – 80 °C until further processing. Sample was further fractionated by high pH reversed-phase chromatography using Agilent 1260 HPLC (Agilent, Santa Clara, CA) and Waters

xbridge column (c18 4.6 x 150mm, 3.5 μ m). 90 fractions were collected and combined into 10 fractions, followed by desalting using Nestgroup c18 tips (Southborough, MA). Fractionated peptides were dried and redissolved in 0.1% FA for LC–MS/MS analysis. Fractions were run on Thermo Fisher Orbitrap Velos Pro coupled with Agilent NanoLC system (Agilent, Santa Clara, CA) over a 60 min gradient. The LC columns (15 cm \times 75 μ m ID, Zorbax 300SB-C18) were purchased from Agilent. Samples were analyzed with a 60-minute linear gradient (0–35% acetonitrile with 0.1% formic acid) and data were acquired in a data dependent manner, in which MS/MS fragmentation is performed on top 12 intense peaks of every full MS scan. RAW files were converted into .mgf files using MSConvert (from ProteoWizard). Database search was carried out using Mascot server (from Matrix Science). Search results from 18 runs were imported into Scaffold (Proteome Software, Portland, OR) for quantitative analysis.

BIBLIOGRAPHY

- 1 Silhavy, T. J., Kahne, D. & Walker, S. The bacterial cell envelope. *Cold Spring Harb Perspect Biol* **2**, a000414, doi:10.1101/cshperspect.a000414 (2010).
- 2 Brown, S., Santa Maria, J. P., Jr. & Walker, S. Wall teichoic acids of gram-positive bacteria. *Annu Rev Microbiol* **67**, 313-336, doi:10.1146/annurev-micro-092412-155620 (2013).
- 3 Neuhaus, F. C. & Baddiley, J. A continuum of anionic charge: structures and functions of D-alanyl-teichoic acids in gram-positive bacteria. *Microbiol Mol Biol Rev* **67**, 686-723, doi:10.1128/MMBR.67.4.686-723.2003 (2003).
- 4 Green, E. R. & Meccas, J. Bacterial Secretion Systems: An Overview. *Microbiol Spectr* **4**, doi:10.1128/microbiolspec.VMBF-0012-2015 (2016).
- 5 Lenz, L. L., Mohammadi, S., Geissler, A. & Portnoy, D. A. SecA2-dependent secretion of autolytic enzymes promotes *Listeria monocytogenes* pathogenesis. *Proc Natl Acad Sci U S A* **100**, 12432-12437, doi:10.1073/pnas.2133653100 (2003).
- 6 Berg, K. H., Stamsas, G. A., Straume, D. & Havarstein, L. S. Effects of low PBP2b levels on cell morphology and peptidoglycan composition in *Streptococcus pneumoniae* R6. *J Bacteriol* **195**, 4342-4354, doi:10.1128/JB.00184-13 (2013).
- 7 Thonnings, S. *et al.* Antibiotic treatment and mortality in patients with *Listeria monocytogenes* meningitis or bacteraemia. *Clin Microbiol Infect* **22**, 725-730, doi:10.1016/j.cmi.2016.06.006 (2016).
- 8 Freitag, N. E., Port, G. C. & Miner, M. D. *Listeria monocytogenes* - from saprophyte to intracellular pathogen. *Nat Rev Microbiol* **7**, 623-628, doi:10.1038/nrmicro2171 (2009).

- 9 Radoshevich, L. & Cossart, P. *Listeria monocytogenes*: towards a complete picture of its physiology and pathogenesis. *Nat Rev Microbiol* **16**, 32-46, doi:10.1038/nrmicro.2017.126 (2018).
- 10 Vazquez-Boland, J. A. *et al.* *Listeria* pathogenesis and molecular virulence determinants. *Clin Microbiol Rev* **14**, 584-640, doi:10.1128/CMR.14.3.584-640.2001 (2001).
- 11 CDC. *Antibiotic Resistance, Food, and Food Animals*, <<https://www.cdc.gov/foodsafety/challenges/antibiotic-resistance.html>> (2020).
- 12 Liu, H. *et al.* PrsA contributes to *Streptococcus suis* serotype 2 pathogenicity by modulating secretion of selected virulence factors. *Vet Microbiol* **236**, 108375, doi:10.1016/j.vetmic.2019.07.027 (2019).
- 13 Nguyen, C. T., Park, S. S. & Rhee, D. K. Stress responses in *Streptococcus* species and their effects on the host. *J Microbiol* **53**, 741-749, doi:10.1007/s12275-015-5432-6 (2015).
- 14 Collaborators, G. L. Estimates of the global, regional, and national morbidity, mortality, and aetiologies of lower respiratory tract infections in 195 countries: a systematic analysis for the Global Burden of Disease Study 2015. *Lancet Infect Dis* **17**, 1133-1161, doi:10.1016/S1473-3099(17)30396-1 (2017).
- 15 Brooks, L. R. K. & Mias, G. I. *Streptococcus pneumoniae*'s Virulence and Host Immunity: Aging, Diagnostics, and Prevention. *Front Immunol* **9**, 1366, doi:10.3389/fimmu.2018.01366 (2018).
- 16 Control, C. f. D. U. (2019).
- 17 Huang, S. S. *et al.* Healthcare utilization and cost of pneumococcal disease in the United States. *Vaccine* **29**, 3398-3412, doi:10.1016/j.vaccine.2011.02.088 (2011).

- 18 Weycker, D. *et al.* Rates and costs of invasive pneumococcal disease and pneumonia in persons with underlying medical conditions. *BMC Health Serv Res* **16**, 182, doi:10.1186/s12913-016-1432-4 (2016).
- 19 Aminov, R. I. A brief history of the antibiotic era: lessons learned and challenges for the future. *Front Microbiol* **1**, 134, doi:10.3389/fmicb.2010.00134 (2010).
- 20 Lozano, C. & Torres, C. [Update on antibiotic resistance in Gram-positive bacteria]. *Enferm Infecc Microbiol Clin* **35 Suppl 1**, 2-8, doi:10.1016/S0213-005X(17)30028-9 (2017).
- 21 Ventola, C. L. The antibiotic resistance crisis: part 1: causes and threats. *P T* **40**, 277-283 (2015).
- 22 Davies, J. Origins and evolution of antibiotic resistance. *Microbiologia* **12**, 9-16 (1996).
- 23 Rasko, D. A. & Sperandio, V. Anti-virulence strategies to combat bacteria-mediated disease. *Nat Rev Drug Discov* **9**, 117-128, doi:10.1038/nrd3013 (2010).
- 24 Scheuplein, N. J. *et al.* Targeting Protein Folding: A Novel Approach for the Treatment of Pathogenic Bacteria. *J Med Chem* **63**, 13355-13388, doi:10.1021/acs.jmedchem.0c00911 (2020).
- 25 Chao, S. H., Greenleaf, A. L. & Price, D. H. Juglone, an inhibitor of the peptidyl-prolyl isomerase Pin1, also directly blocks transcription. *Nucleic Acids Res* **29**, 767-773, doi:10.1093/nar/29.3.767 (2001).
- 26 Saibil, H. Chaperone machines for protein folding, unfolding and disaggregation. *Nat Rev Mol Cell Biol* **14**, 630-642, doi:10.1038/nrm3658 (2013).

- 27 Unal, C. M. & Steinert, M. Microbial peptidyl-prolyl cis/trans isomerases (PPIases): virulence factors and potential alternative drug targets. *Microbiol Mol Biol Rev* **78**, 544-571, doi:10.1128/MMBR.00015-14 (2014).
- 28 Crowley, P. J. & Brady, L. J. Evaluation of the effects of *Streptococcus mutans* chaperones and protein secretion machinery components on cell surface protein biogenesis, competence, and mutacin production. *Mol Oral Microbiol* **31**, 59-77, doi:10.1111/omi.12130 (2016).
- 29 Davis, T. L. *et al.* Structural and biochemical characterization of the human cyclophilin family of peptidyl-prolyl isomerases. *PLoS Biol* **8**, e1000439, doi:10.1371/journal.pbio.1000439 (2010).
- 30 Hotze, E. M. & Tweten, R. K. Membrane assembly of the cholesterol-dependent cytolysin pore complex. *Biochim Biophys Acta* **1818**, 1028-1038, doi:10.1016/j.bbamem.2011.07.036 (2012).
- 31 Hsu, C. C. *et al.* *Streptococcus mutans* PrsA mediates AtIA secretion contributing to extracellular DNA release and biofilm formation in the pathogenesis of infective endocarditis. *Virulence* **13**, 1379-1392, doi:10.1080/21505594.2022.2105351 (2022).
- 32 Price, K. E. & Camilli, A. Pneumolysin localizes to the cell wall of *Streptococcus pneumoniae*. *J Bacteriol* **191**, 2163-2168, doi:10.1128/JB.01489-08 (2009).
- 33 Price, K. E., Greene, N. G. & Camilli, A. Export requirements of pneumolysin in *Streptococcus pneumoniae*. *J Bacteriol* **194**, 3651-3660, doi:10.1128/JB.00114-12 (2012).
- 34 Gerard, M., Deleersnijder, A., Demeulemeester, J., Debyser, Z. & Baekelandt, V. Unraveling the role of peptidyl-prolyl isomerases in neurodegeneration. *Mol Neurobiol* **44**, 13-27, doi:10.1007/s12035-011-8184-2 (2011).

- 35 Gothel, S. F., Scholz, C., Schmid, F. X. & Marahiel, M. A. Cyclophilin and trigger factor from *Bacillus subtilis* catalyze in vitro protein folding and are necessary for viability under starvation conditions. *Biochemistry* **37**, 13392-13399, doi:10.1021/bi981253w (1998).
- 36 Arora, K. *et al.* Extracellular cyclophilins contribute to the regulation of inflammatory responses. *J Immunol* **175**, 517-522, doi:10.4049/jimmunol.175.1.517 (2005).
- 37 Schiene-Fischer, C., Aumuller, T. & Fischer, G. Peptide bond cis/trans isomerases: a biocatalysis perspective of conformational dynamics in proteins. *Top Curr Chem* **328**, 35-67, doi:10.1007/128_2011_151 (2013).
- 38 Soderberg, M. A. & Cianciotto, N. P. A *Legionella pneumophila* peptidyl-prolyl cis-trans isomerase present in culture supernatants is necessary for optimal growth at low temperatures. *Appl Environ Microbiol* **74**, 1634-1638, doi:10.1128/AEM.02512-07 (2008).
- 39 Gioti, A. *et al.* Expression profiling of *Botrytis cinerea* genes identifies three patterns of up-regulation in planta and an FKBP12 protein affecting pathogenicity. *J Mol Biol* **358**, 372-386, doi:10.1016/j.jmb.2006.01.076 (2006).
- 40 Reyes, D. Y. & Yoshikawa, H. DnaK chaperone machine and trigger factor are only partially required for normal growth of *Bacillus subtilis*. *Biosci Biotechnol Biochem* **66**, 1583-1586, doi:10.1271/bbb.66.1583 (2002).
- 41 Bigot, A., Botton, E., Dubail, I. & Charbit, A. A homolog of *Bacillus subtilis* trigger factor in *Listeria monocytogenes* is involved in stress tolerance and bacterial virulence. *Appl Environ Microbiol* **72**, 6623-6631, doi:10.1128/AEM.00624-06 (2006).
- 42 Tremillon, N. *et al.* PpiA, a surface PPIase of the cyclophilin family in *Lactococcus lactis*. *PLoS One* **7**, e33516, doi:10.1371/journal.pone.0033516 (2012).

- 43 Mukouhara, T., Arimoto, T., Cho, K., Yamamoto, M. & Igarashi, T. Surface lipoprotein PpiA of *Streptococcus mutans* suppresses scavenger receptor MARCO-dependent phagocytosis by macrophages. *Infect Immun* **79**, 4933-4940, doi:10.1128/IAI.05693-11 (2011).
- 44 Hayano, T., Takahashi, N., Kato, S., Maki, N. & Suzuki, M. Two distinct forms of peptidylprolyl-cis-trans-isomerase are expressed separately in periplasmic and cytoplasmic compartments of *Escherichia coli* cells. *Biochemistry* **30**, 3041-3048, doi:10.1021/bi00226a009 (1991).
- 45 Hermans, P. W. *et al.* The streptococcal lipoprotein rotamase A (SlrA) is a functional peptidyl-prolyl isomerase involved in pneumococcal colonization. *J Biol Chem* **281**, 968-976, doi:10.1074/jbc.M510014200 (2006).
- 46 Cahoon, L. A. & Freitag, N. E. *Listeria monocytogenes* virulence factor secretion: don't leave the cell without a chaperone. *Front Cell Infect Microbiol* **4**, 13, doi:10.3389/fcimb.2014.00013 (2014).
- 47 Alonzo, F., 3rd, Port, G. C., Cao, M. & Freitag, N. E. The posttranslocation chaperone PrsA2 contributes to multiple facets of *Listeria monocytogenes* pathogenesis. *Infect Immun* **77**, 2612-2623, doi:10.1128/IAI.00280-09 (2009).
- 48 Heitman, J., Movva, N. R., Hiestand, P. C. & Hall, M. N. FK 506-binding protein proline rotamase is a target for the immunosuppressive agent FK 506 in *Saccharomyces cerevisiae*. *Proc Natl Acad Sci U S A* **88**, 1948-1952, doi:10.1073/pnas.88.5.1948 (1991).
- 49 Xu, X. *et al.* FKBP12 is the only FK506 binding protein mediating T-cell inhibition by the immunosuppressant FK506. *Transplantation* **73**, 1835-1838, doi:10.1097/00007890-200206150-00023 (2002).

- 50 Wang, P. & Heitman, J. The cyclophilins. *Genome Biol* **6**, 226, doi:10.1186/gb-2005-6-7-226 (2005).
- 51 Dourlen, P. *et al.* The peptidyl prolyl cis/trans isomerase Pin1 downregulates the Inhibitor of Apoptosis Protein Survivin. *Biochim Biophys Acta* **1773**, 1428-1437, doi:10.1016/j.bbamcr.2007.05.012 (2007).
- 52 Wiemels, R. E. *et al.* An Intracellular Peptidyl-Prolyl cis/trans Isomerase Is Required for Folding and Activity of the Staphylococcus aureus Secreted Virulence Factor Nuclease. *J Bacteriol* **199**, doi:10.1128/JB.00453-16 (2017).
- 53 Unal, C. M. *et al.* Pleiotropic Clostridioides difficile Cyclophilin PpiB Controls Cysteine-Tolerance, Toxin Production, the Central Metabolism and Multiple Stress Responses. *Front Pharmacol* **10**, 340, doi:10.3389/fphar.2019.00340 (2019).
- 54 Jiang, B. & Pei, D. A Selective, Cell-Permeable Nonphosphorylated Bicyclic Peptidyl Inhibitor against Peptidyl-Prolyl Isomerase Pin1. *J Med Chem* **58**, 6306-6312, doi:10.1021/acs.jmedchem.5b00411 (2015).
- 55 Hennig, L. *et al.* Selective inactivation of parvulin-like peptidyl-prolyl cis/trans isomerases by juglone. *Biochemistry* **37**, 5953-5960, doi:10.1021/bi973162p (1998).
- 56 Cron, L. E. *et al.* Surface-associated lipoprotein PpmA of Streptococcus pneumoniae is involved in colonization in a strain-specific manner. *Microbiology (Reading)* **155**, 2401-2410, doi:10.1099/mic.0.026765-0 (2009).
- 57 Jakob, R. P. *et al.* Dimeric Structure of the Bacterial Extracellular Foldase PrsA. *J Biol Chem* **290**, 3278-3292, doi:10.1074/jbc.M114.622910 (2015).

- 58 Hyyrylainen, H. L. *et al.* Penicillin-binding protein folding is dependent on the PrsA peptidyl-prolyl cis-trans isomerase in *Bacillus subtilis*. *Mol Microbiol* **77**, 108-127, doi:10.1111/j.1365-2958.2010.07188.x (2010).
- 59 Alonzo, F., 3rd, Xayarath, B., Whisstock, J. C. & Freitag, N. E. Functional analysis of the *Listeria monocytogenes* secretion chaperone PrsA2 and its multiple contributions to bacterial virulence. *Mol Microbiol* **80**, 1530-1548, doi:10.1111/j.1365-2958.2011.07665.x (2011).
- 60 Cahoon, L. A., Freitag, N. E. & Prehna, G. A structural comparison of *Listeria monocytogenes* protein chaperones PrsA1 and PrsA2 reveals molecular features required for virulence. *Mol Microbiol* **101**, 42-61, doi:10.1111/mmi.13367 (2016).
- 61 Alonzo, F., 3rd & Freitag, N. E. *Listeria monocytogenes* PrsA2 is required for virulence factor secretion and bacterial viability within the host cell cytosol. *Infect Immun* **78**, 4944-4957, doi:10.1128/IAI.00532-10 (2010).
- 62 Cahoon, L. A. *et al.* *Listeria monocytogenes* two component system PieRS regulates secretion chaperones PrsA1 and PrsA2 and enhances bacterial translocation across the intestine. *Mol Microbiol* **118**, 278-293, doi:10.1111/mmi.14967 (2022).
- 63 Overweg, K. *et al.* The putative proteinase maturation protein A of *Streptococcus pneumoniae* is a conserved surface protein with potential to elicit protective immune responses. *Infect Immun* **68**, 4180-4188, doi:10.1128/IAI.68.7.4180-4188.2000 (2000).
- 64 Cahoon, L. A. & Freitag, N. E. Identification of Conserved and Species-Specific Functions of the *Listeria monocytogenes* PrsA2 Secretion Chaperone. *Infect Immun* **83**, 4028-4041, doi:10.1128/IAI.00504-15 (2015).

- 65 Guo, L. *et al.* Phenotypic characterization of the foldase homologue PrsA in *Streptococcus mutans*. *Mol Oral Microbiol* **28**, 154-165, doi:10.1111/omi.12014 (2013).
- 66 Port, G. C. & Freitag, N. E. Identification of novel *Listeria monocytogenes* secreted virulence factors following mutational activation of the central virulence regulator, PrfA. *Infect Immun* **75**, 5886-5897, doi:10.1128/IAI.00845-07 (2007).
- 67 Bitto, E. & McKay, D. B. Crystallographic structure of SurA, a molecular chaperone that facilitates folding of outer membrane porins. *Structure* **10**, 1489-1498, doi:10.1016/s0969-2126(02)00877-8 (2002).
- 68 Baumgartner, M. *et al.* Inactivation of Lgt allows systematic characterization of lipoproteins from *Listeria monocytogenes*. *J Bacteriol* **189**, 313-324, doi:10.1128/JB.00976-06 (2007).
- 69 Kontinen, V. P. & Sarvas, M. The PrsA lipoprotein is essential for protein secretion in *Bacillus subtilis* and sets a limit for high-level secretion. *Mol Microbiol* **8**, 727-737, doi:10.1111/j.1365-2958.1993.tb01616.x (1993).
- 70 Jacobs, M., Andersen, J. B., Kontinen, V. & Sarvas, M. *Bacillus subtilis* PrsA is required in vivo as an extracytoplasmic chaperone for secretion of active enzymes synthesized either with or without pro-sequences. *Mol Microbiol* **8**, 957-966, doi:10.1111/j.1365-2958.1993.tb01640.x (1993).
- 71 Nishimoto, A. T., Rosch, J. W. & Tuomanen, E. I. Pneumolysin: Pathogenesis and Therapeutic Target. *Front Microbiol* **11**, 1543, doi:10.3389/fmicb.2020.01543 (2020).
- 72 Zemansky, J. *et al.* Development of a mariner-based transposon and identification of *Listeria monocytogenes* determinants, including the peptidyl-prolyl isomerase PrsA2, that

- contribute to its hemolytic phenotype. *J Bacteriol* **191**, 3950-3964, doi:10.1128/JB.00016-09 (2009).
- 73 Ireton, K., Mortuza, R., Gyanwali, G. C., Gianfelice, A. & Hussain, M. Role of internalin proteins in the pathogenesis of *Listeria monocytogenes*. *Mol Microbiol* **116**, 1407-1419, doi:10.1111/mmi.14836 (2021).
- 74 Mirdita, M. *et al.* ColabFold: making protein folding accessible to all. *Nat Methods* **19**, 679-682, doi:10.1038/s41592-022-01488-1 (2022).
- 75 Lechuga, S. & Ivanov, A. I. Disruption of the epithelial barrier during intestinal inflammation: Quest for new molecules and mechanisms. *Biochim Biophys Acta Mol Cell Res* **1864**, 1183-1194, doi:10.1016/j.bbamcr.2017.03.007 (2017).
- 76 Polle, L., Rigano, L. A., Julian, R., Ireton, K. & Schubert, W. D. Structural details of human tuba recruitment by InlC of *Listeria monocytogenes* elucidate bacterial cell-cell spreading. *Structure* **22**, 304-314, doi:10.1016/j.str.2013.10.017 (2014).
- 77 Rajabian, T. *et al.* The bacterial virulence factor InlC perturbs apical cell junctions and promotes cell-to-cell spread of *Listeria*. *Nat Cell Biol* **11**, 1212-1218, doi:10.1038/ncb1964 (2009).
- 78 Parker, D. *et al.* The NanA neuraminidase of *Streptococcus pneumoniae* is involved in biofilm formation. *Infect Immun* **77**, 3722-3730, doi:10.1128/IAI.00228-09 (2009).
- 79 Hammond, A. J. *et al.* Neuraminidase B controls neuraminidase A-dependent mucus production and evasion. *PLoS Pathog* **17**, e1009158, doi:10.1371/journal.ppat.1009158 (2021).

- 80 Van de Velde, S. *et al.* Penicillin-binding proteins (PBP) and Lmo0441 (a PBP-like protein) play a role in Beta-lactam sensitivity of *Listeria monocytogenes*. *Gut Pathog* **1**, 23, doi:10.1186/1757-4749-1-23 (2009).
- 81 Jumper, J. *et al.* Highly accurate protein structure prediction with AlphaFold. *Nature* **596**, 583-589, doi:10.1038/s41586-021-03819-2 (2021).
- 82 Steinegger, M. & Soding, J. MMseqs2 enables sensitive protein sequence searching for the analysis of massive data sets. *Nat Biotechnol* **35**, 1026-1028, doi:10.1038/nbt.3988 (2017).
- 83 Evans, R. *et al.* Protein complex prediction with AlphaFold-Multimer. *bioRxiv*, 2021.2010.2004.463034, doi:10.1101/2021.10.04.463034 (2022).
- 84 Jousselin, E. *et al.* Assessment of a 16S rRNA amplicon Illumina sequencing procedure for studying the microbiome of a symbiont-rich aphid genus. *Mol Ecol Resour* **16**, 628-640, doi:10.1111/1755-0998.12478 (2016).
- 85 Drouault, S. *et al.* The peptidyl-prolyl isomerase motif is lacking in PmpA, the PrsA-like protein involved in the secretion machinery of *Lactococcus lactis*. *Appl Environ Microbiol* **68**, 3932-3942, doi:10.1128/AEM.68.8.3932-3942.2002 (2002).
- 86 Wu, Z. Y. *et al.* Unique virulence role of post-translocational chaperone PrsA in shaping *Streptococcus pyogenes* secretome. *Virulence* **12**, 2633-2647, doi:10.1080/21505594.2021.1982501/SUPPL_FILE/KVIR_A_1982501_SM3960.ZIP (2021).
- 87 Heikkinen, O. *et al.* Solution structure of the parvulin-type PPIase domain of *Staphylococcus aureus* PrsA--implications for the catalytic mechanism of parvulins. *BMC Struct Biol* **9**, 17, doi:10.1186/1472-6807-9-17 (2009).

- 88 Vitikainen, M. *et al.* Structure-function analysis of PrsA reveals roles for the parvulin-like and flanking N- and C-terminal domains in protein folding and secretion in *Bacillus subtilis*. *J Biol Chem* **279**, 19302-19314, doi:10.1074/jbc.M400861200 (2004).
- 89 Thoma, J., Burmann, B. M., Hiller, S. & Muller, D. J. Impact of holdase chaperones Skp and SurA on the folding of beta-barrel outer-membrane proteins. *Nat Struct Mol Biol* **22**, 795-802, doi:10.1038/nsmb.3087 (2015).
- 90 Alonzo III, F. & Freitag, N. E. *Listeria monocytogenes* PrsA2 is required for virulence factor secretion and bacterial viability within the host cell cytosol. *Infection and immunity* **78**, 4944-4957 (2010).
- 91 Cahoon, L. A. *et al.* *Listeria monocytogenes* two component system PieRS regulates secretion chaperones PrsA1 and PrsA2 and enhances bacterial translocation across the intestine. *Molecular microbiology* **118**, 278-293 (2022).
- 92 Cahoon, L. A. & Freitag, N. E. Identification of conserved and species-specific functions of the *Listeria monocytogenes* PrsA2 secretion chaperone. *Infection and Immunity* **83**, 4028-4041, doi:10.1128/IAI.00504-15 (2015).
- 93 Alonzo, F., Xayarath, B., Whisstock, J. C. & Freitag, N. E. Functional analysis of the *Listeria monocytogenes* secretion chaperone PrsA2 and its multiple contributions to bacterial virulence. *Molecular Microbiology* **80**, 1530-1548, doi:10.1111/j.1365-2958.2011.07665.x (2011).
- 94 Walters, W. P. Going further than Lipinski's rule in drug design. *Expert Opin Drug Discov* **7**, 99-107, doi:10.1517/17460441.2012.648612 (2012).

- 95 Jerabek-Willemsen, M., Wienken, C. J., Braun, D., Baaske, P. & Duhr, S. Molecular interaction studies using microscale thermophoresis. *Assay Drug Dev Technol* **9**, 342-353, doi:10.1089/adt.2011.0380 (2011).
- 96 Linke, P. *et al.* An Automated Microscale Thermophoresis Screening Approach for Fragment-Based Lead Discovery. *J Biomol Screen* **21**, 414-421, doi:10.1177/1087057115618347 (2016).
- 97 Rainard, J. M., Pandarakalam, G. C. & McElroy, S. P. Using Microscale Thermophoresis to Characterize Hits from High-Throughput Screening: A European Lead Factory Perspective. *SLAS Discov* **23**, 225-241, doi:10.1177/2472555217744728 (2018).
- 98 Schiebel, J. *et al.* One Question, Multiple Answers: Biochemical and Biophysical Screening Methods Retrieve Deviating Fragment Hit Lists. *ChemMedChem* **10**, 1511-1521, doi:10.1002/cmdc.201500267 (2015).
- 99 Schiebel, J. *et al.* Six Biophysical Screening Methods Miss a Large Proportion of Crystallographically Discovered Fragment Hits: A Case Study. *ACS Chem Biol* **11**, 1693-1701, doi:10.1021/acscchembio.5b01034 (2016).